

1
2
3
4
5
6
7
8
9
10
11
12
13
14
15
16
17
18
19
20
21
22
23
24
25
26
27
28
29
30
31
32
33
34
35
36
37
38
39
40
41
42
43
44
45

HIV-1 Vpr Inhibits Kaposi's Sarcoma-Associated Herpesvirus Lytic Replication by Inducing MiR-942-5p and Activating NF-κB Signaling

Qin Yan,^{1,2,3} Chenyou Shen,⁴ Jie Qin,³ Wan Li,³ Minmin Hu,³ Hongmei Lu,⁵ Di Qin,³ Jianzhong Zhu,⁶ Shou-Jiang Gao⁷ and Chun Lu^{1,2,3*}

¹ State Key Laboratory of Reproductive Medicine, Nanjing Medical University, Nanjing 210029, P. R. China

² Key Laboratory of Pathogen Biology of Jiangsu Province, Nanjing Medical University, Nanjing 210029, P. R. China

³ Department of Microbiology, Nanjing Medical University, Nanjing 210029, P. R. China

⁴ Jiangsu Key Laboratory of Organ Transplantation, Wuxi People's Hospital, Nanjing Medical University, Wuxi 214000, P. R. China

⁵ Department of Obstetrics, the First Affiliated Hospital of Nanjing Medical University, Nanjing 210029, P.R. China

⁶ College of Veterinary Medicine, Yangzhou University, Yangzhou 225009, P. R. China

⁷ Department of Molecular Microbiology and Immunology, Keck School of Medicine, University of Southern California, Los Angeles, CA 90033, USA

Running Title: MiR-942/NF-κB Axis Regulates Vpr Inhibition of KSHV Lytic Replication

Key words: KSHV; Latency and reactivation; MicroRNAs; HIV-1 Vpr; NF-κB signaling

46
47
48
49
50
51
52
53
54
55
56
57
58
59
60
61
62
63
64
65
66
67
68
69
70
71
72
73
74
75
76
77
78
79
80
81

*Corresponding author:

Dr. Chun Lu. Mailing address: Department of Microbiology, Nanjing Medical University,
Nanjing, 210029, P. R. China, Phone: 86-25-86862910. Fax: 86-25-86508960. Email:
clu@njmu.edu.cn

The word count of the Abstract: 199

The number of figures: 8

The number of tables: 1

Abstract

Kaposi's sarcoma-associated herpesvirus (KSHV) infection is required for the development of several AIDS-related malignancies, including Kaposi's sarcoma (KS) and primary effusion lymphoma (PEL). The high incidence of AIDS-KS has been ascribed to the interaction of KSHV and HIV-1. We have previously shown that HIV-1 secreted proteins, Tat and Nef, regulate KSHV lifecycle, and synergize with KSHV oncogenes to promote angiogenesis and tumorigenesis. Here, we examined the regulation of KSHV latency by HIV-1 viral protein R (Vpr). We found that soluble Vpr inhibits the expression of KSHV lytic transcripts and proteins, as well as viral particle production by activating NF- κ B signaling following internalization into PEL cells. By analyzing the expression profiles of microRNAs combined with target search by bioinformatics and luciferase reporter analyses, we identified a Vpr-upregulated cellular microRNA (miRNA), miR-942-5p, that directly targeted I κ B α . Suppression of miR-942-5p relieved the expression of I κ B α and reduced Vpr inhibition of KSHV lytic replication while overexpression of miR-942-5p enhanced Vpr inhibition of KSHV lytic replication. Our findings collectively illustrate that, by activating NF- κ B signaling through upregulating a cellular miRNA to target I κ B α , internalized HIV-1 Vpr inhibits KSHV lytic replication. These results have demonstrated an essential role of Vpr in the lifecycle of KSHV.

105
106
107
108
109
110
111
112
113
114
115
116
117
118
119
120
121
122
123
124
125
126
127

Importance

Co-infection by HIV-1 promotes the aggressive growth of Kaposi's sarcoma-associated herpesvirus (KSHV)-related malignancies, including Kaposi's sarcoma (KS) and primary effusion lymphoma (PEL). In this study, we have shown that soluble HIV-1 Vpr inhibits KSHV lytic replication by activating NF- κ B signaling following internalization into PEL cells. Mechanistic studies revealed that a cellular microRNA upregulated by Vpr, miR-942-5p, directly targeted I κ B α . Suppression of miR-942-5p relieved I κ B α expression and reduced Vpr inhibition of KSHV replication while overexpression of miR-942-5p enhanced Vpr inhibition of KSHV replication. These results indicate that, by activating NF- κ B signaling through upregulating a cellular miRNA to target I κ B α , internalized Vpr inhibits KSHV lytic replication. This work illustrates a molecular mechanism by which HIV-1 secreted regulatory protein Vpr regulates KSHV latency and pathogenesis of AIDS-related malignancies.

128

129

130 **Introduction**

131 Kaposi's sarcoma-associated herpesvirus (KSHV), also known as human herpesvirus
132 8 (HHV-8), is the causative agent of Kaposi's sarcoma (KS). AIDS-associated Kaposi's
133 sarcoma (AIDS-KS) remains a clinical challenge in sub-Saharan Africa and United States
134 including a subset of AIDS patients receiving highly active antiretroviral therapy
135 (HAART)(1-4). KSHV infection is also linked to two B-cell lymphoproliferative disorders
136 associated with AIDS including primary effusion lymphoma (PEL) and a subset of
137 multicentric Castleman's disease (MCD)(5, 6).

138 KSHV displays two distinct replication phases: a latent phase and a productive lytic
139 phase. Following acute infection, KSHV in general establishes lifetime persistence in the
140 infected individuals. During the latent phase, only a limited number of viral genes are
141 expressed, which serve to maintain the persistence of viral genome, restrict host immune
142 responses and enhance cell survival. KSHV latently infected cells can be reactivated into
143 lytic replication by several intracellular or extracellular stimuli, such as hypoxia, oxidative
144 stress, and certain cytokines (7-10). Activation of viral lytic replication results in the
145 expression of viral lytic genes and production of infectious virions (11). Both latent and lytic
146 replication phases are crucial for the long-term persistence of KSHV in the host, and their
147 gene products play critical roles in the pathogenesis of KSHV-associated disease.

148 Like other human oncogenic viruses, KSHV infection alone is not sufficient to cause
149 KSHV-associated malignancy (1, 12). Previously, we and others have demonstrated that
150 other co-factors, such as human herpesvirus 6 (HHV-6), herpes simplex virus type 1

151 (HSV-1), human immunodeficiency virus type 1 (HIV-1) and human cytomegalovirus
152 (HCMV) regulate the lifecycle of KSHV and cell proliferation and survival, thus might
153 contribute to the development of these malignancies (13-17). Among these co-factors,
154 HIV-1 infection increases KS incidence in HIV-infected individuals (3). However, HIV-1 and
155 KSHV do not infect the same cell type (18), implying an indirect role of HIV-1 in AIDS-KS.
156 Current evidence strongly supports that HIV-1 might promote the initiation and progression
157 of KS by inducing inflammatory cytokines and producing secreted regulatory proteins in
158 addition to inducing immunosuppression. HIV-1 transactivator of transcription (Tat) and
159 negative factor (Nef) are released into the bloodstream from HIV infected cells, which
160 contribute to the pathogenesis of AIDS-related malignancies (19, 20). Recently, we and
161 others have demonstrated that Tat can not only trigger KSHV reactivation from latency (21)
162 but also accelerate tumor progression induced by KSHV-encoded oncoproteins, including
163 the viral G protein-coupled receptor (vGPCR), Kaposin A, viral interleukin-6 (vIL-6) and
164 ORF K1 (22-25). Moreover, we have found that soluble Nef can be readily internalized by
165 PEL cells and endothelial cells, and both soluble and ectopic expression of Nef promote
166 KSHV latency by inhibiting viral replication, and induce angiogenesis and oncogenesis by
167 cooperating with KSHV vIL-6 or ORF K1 (26-28).

168 Besides Tat and Nef, viral protein R (Vpr) is another HIV-1 accessory protein, which is
169 a virion-associated nuclear protein of ~15 kDa (29). Vpr exhibits a variety of biological
170 functions including nuclear localization of pre-integration complex (PIC) (30), G2/M cell
171 cycle arrest (31, 32), transactivation of HIV-1 long terminal repeat (LTR) (33) and induction
172 of apoptosis (34). Importantly, Vpr can be found *in vivo* in an extracellular soluble form.
173 Indeed, despite it is an intracellular or intravirion protein, Vpr has been detected as a

174 soluble protein in the sera and cerebrospinal fluid (CSF) of HIV-1-infected patients (35-37),
175 as well as in the extracellular medium of virus-producing cells *in vitro* (38).

176 In this study, we have demonstrated a role of HIV-1 Vpr in controlling the balance
177 between KSHV lytic replication and latency. We found that soluble Vpr regulates KSHV
178 latency via activation of the nuclear factor-kappaB (NF- κ B) signaling following
179 internalization into the PEL cells. Furthermore, a cellular microRNA (miRNA), miR-942-5p,
180 was identified to mediate Vpr inhibition of KSHV replication by directly targeting the inhibitor
181 of NF- κ B (I κ B α). This work reveals the involvement of Vpr in KSHV life cycle and the
182 molecular mechanisms of regulation of KSHV replication program and pathogenesis of
183 AIDS-related malignancies by HIV-1 secreted regulatory proteins.

184

185

186

187

188

189

190

191

192

193

194

195

196

197 **Materials and Methods**

198 **Cells Culture, Plasmids and Transfection:** EBV-negative and KSHV-positive PEL cell
199 lines (BC3 cells and BCBL-1 cells) and HEK293T cells were cultured in RPMI-1640 and
200 Dulbecco's Modified Eagle's Medium (DMEM), respectively, both of which contained 10%
201 inactivated fetal bovine serum (FBS), 2 mM L-glutamine, 100 U/ml penicillin, and 100 µg/ml
202 streptomycin at 37°C in a humidified, 5% CO₂ atmosphere.

203 The NF-κB reporter plasmid containing three tandem repeats of consensus NF-κB
204 binding sites, IκB dominant negative plasmid (IκB-DN) obtained by cloning into lentiviral
205 pCDH vectors with Flag tag, and the wild type pGL-3-IκB-3'UTR (WT IκB) plasmid obtained
206 by cloning IκB 3'UTR into the downstream of pGL-3 Control luciferase reporter vector were
207 prepared as described previously (39). HIV-1 LTR luciferase reporter construct was kindly
208 provided by Zan Huang (Wuhan University, China). Target prediction software PITA,
209 RNAhybrid and RNA22 were used to analyze the binding sites of miR-942-5p in IκB 3'UTR.
210 The pGL-3-IκB-3'UTR mutant plasmid (mut IκB) with mutated binding sites was made by
211 site-directed mutagenesis. LipofectamineTM 2000 transfection reagent (Invitrogen, Carlsbad,
212 CA, USA) was utilized according to manufacturer's instructions.

213

214 **Preparation of Soluble Vpr Protein (sVpr):** The HIV-1 Vpr gene was ligated into the *Nde* I
215 and *Xba* I sites of the pColdII vector (TaKaRa Biotechnology Co. Ltd, Dalian, China) with
216 the 6XHis tag sequence fused at the N-terminus. The Vpr protein was produced in the
217 *Escherichia coli* BL21 (DE3) Codon (+) RIL strain (TIANGEN Biotech Co. Ltd, Beijing,
218 China) by induction with isopropyl-β-D-thiogalactopyranoside (IPTG; Nacalai Tesque, Inc.,
219 Kyoto, Japan) and was purified as described previously (40). Endotoxin was removed from

220 eluted proteins with the ToxinEraser Endotoxin Removal procedure (GenScript) (41). The
221 cells producing the Vpr protein were suspended in phosphate buffer saline (PBS) and
222 disrupted by sonication. The cell debris was removed by centrifugation for 15 min at 12,000
223 g, and the lysate containing the soluble Vpr protein was mixed gently with Ni-NTA beads
224 (Invitrogen Corp., Carlsbad, CA) for affinity chromatography purification and stained with
225 Coomassie Brilliant Blue R-250. The concentration of the purified Vpr protein was
226 determined with a BCA protein assay kit (Bio-Rad Laboratories, Hercules, CA) using bovine
227 serum albumin (BSA) as the standard.

228

229 **Antibodies:** Anti-KSHV ORF65 mouse monoclonal antibody (MAb) were described
230 previously (42). Anti-I κ B α rabbit MAb and anti-Flag M2 rabbit MAb were from Cell Signaling
231 Technology (Beverly, MA). Anti-KSHV vIL-6 rabbit polyclonal antibody (PAb) and anti-KSHV
232 LANA ORF73 rat MAb were from Advanced Biotechnologies, Inc. (Columbia, MD).
233 Anti-NF- κ B p65 rabbit PAb was obtained from Abcam (Cambridge, MA, USA). Anti-Vpr goat
234 PAb, normal goat IgG, horseradish peroxidase (HRP)-conjugated goat anti-mouse and
235 anti-rabbit IgG, and mouse MAb against α -tubulin used to monitor sample loading, were
236 purchased from Santa Cruz Biotechnology (Santa Cruz, Calif.).

237

238 **Western Blot Analysis:** The procedure of Western blot was previously described (14).
239 Densitometry analysis of protein expression levels were determined by Scion Image
240 software (Scion Corporation, Frederick, MD).

241

242 **Real-Time Quantitative Reverse Transcription-PCR (RT-qPCR):** Total RNA was isolated

243 with Trizol reagent (Invitrogen) for RT-qPCR using SYBR Premix Ex Taq™ Kit (TaKaRa
244 Biotechnology Co. Ltd, Dalian, China) according to the manufacturer's instructions. The
245 sequences of specific primers for KSHV lytic transcripts were listed in Table 1 while the
246 Bulge-Loop miR-942-5p primers were synthesized by Ribo Biotechnology (Guangzhou,
247 China). Stem-loop RT-qPCR was performed as previously described for the quantification
248 of miRNAs (43, 44).

249

250 **Confocal Microscopy:** PEL cells (10^4) smeared on chamber slides were incubated with
251 the indicated primary antibodies and the corresponding secondary antibodies-conjugated
252 with Alexa Fluor of fluorescent dyes (Invitrogen). Cellular nucleus was stained with 4',
253 6'-diamidino-2-phenylindole (DAPI) purchased from Beyotime Institute of Biotechnology
254 (China). The stained cells were observed and photographed with a Zeiss Axiovert 200 M
255 epifluorescence microscope (Carl Zeiss, Freistaat Thuringen, Germany).

256

257 **Real-Time PCR Analysis for Viral Copy Number:** Supernatants of PEL cells were
258 collected to detect viral DNA using the High Pure Viral Nucleic Acid Kit (Roche, Germany)
259 according to the manufacturer's instructions. Purified viral DNA was used for real-time
260 DNA-PCR as described previously (45). Primers designed to detect KSHV lytic genes were
261 listed in Table 1.

262

263 **Luciferase Reporter Assay:** In the NF- κ B activity assay, the NF- κ B reporter plasmid and
264 Renilla vector pRL-TK (Promega) were co-transfected into BC3 cells and BCBL-1 cells. In
265 the I κ B 3'UTR luciferase reporter assay, miRNA mimics, I κ B 3'UTR luciferase reporter

266 plasmid (400 ng) and pRL-TK (20 ng) were co-transfected into HEK293T cells for
267 experiments related to miRNAs. In the HIV-1 LTR activity assay, HIV-1 LTR luciferase report
268 plasmid or pGL3 basic construct was co-transfected with pRL-TK into 293T cells incubated
269 with PBS or soluble Vpr at 50, 100 and 200 ng/mL, respectively. Relative luciferase activity
270 was detected by Promega dual-luciferase reporter assay system.

271

272 **ELISA-based NF- κ B/p65 DNA-binding Activity Assay:** Active Motif nuclear extraction kit
273 (Carlsbad, CA, USA) was utilized to extract nuclear protein of PEL cells for the detection of
274 NF- κ B p65 DNA binding activity by TransFactor NF- κ B p65 ELISA Kit (Clontech
275 Laboratories, Mountain View, CA, USA), where competitor oligonucleotides were used as
276 the negative controls to ensure the assay specificity. The absorbance was measured at 630
277 nm using a microplate reader as previously described (16, 25, 46, 47).

278

279 **Apoptosis assay:** Apoptotic cells were detected by propidium iodide (PI) staining and with
280 a fluorescein isothiocyanate (FITC)-Annexin V (AV) Apoptosis Detection Kit (BD
281 Biosciences, San Jose, CA) according to the manufacturer's instructions.

282

283 **MiRNA Microarray Analysis:** Total RNA from BC3 cells incubated with PBS or soluble Vpr
284 for 72 h was isolated with Trizol reagent (Invitrogen) for miRNA microarray analysis as
285 previously described (26, 27).

286

287 **MiRNA Mimic and Inhibitor:** Synthetic miRNAs mimics and inhibitor as well as their
288 negative controls were purchased from Shanghai GenePharma Company (Shanghai,

289 China). The sequences designed for the miR-942-5p mimic and a negative-control were
290 (5'-UCU UCU CUG UUU UGG CCA UGU G-3') and (5'-UUC UCC GAA CGU GUC ACG
291 UTT-3'), respectively.

292

293 **Statistical Analysis:** SPSS version 18.0 was used for the statistical analysis of
294 experimental data. Data are presented as mean \pm standard error of mean (SEM).
295 Differences with $P < 0.05$ were considered statistically significant. All the experiments were
296 repeated three times and each experiment contained at least three replicates, unless
297 otherwise stated.

298

299

300

301

302 **Results**

303 **Internalized soluble Vpr protein inhibits KSHV lytic replication in PEL cells**

304 As a HIV accessory protein that can be released from HIV-1 infected cells, Vpr might
305 be involved in the regulation of KSHV latency as Tat and Nef do (21, 26). The recombinant
306 Vpr (soluble Vpr) was purified by affinity chromatography (Fig. 1A). The purified soluble Vpr
307 activated HIV-1 long terminal repeat (LTR)-driven luciferase activity at as low as 50 ng/ml as
308 previously described (Fig. 1B) (48), indicating that it was functional with the expected
309 biological activity. We treated BC3 cells with 0, 1, 10, 100, 200, and 500 ng/ml of purified
310 soluble Vpr. As shown in Fig. 1C and 1D, soluble Vpr protein did not induce apoptosis in
311 BC3 cells until 500 ng/ml, a concentration 50-fold greater than those found in serum

312 samples from HIV infected patients (1 to 10 ng/mL) (37). Since soluble Vpr protein can be
313 taken up by multiple cell types (36, 49-52), immunofluorescent assay was performed to
314 determine whether it can also be internalized by BC3 cells and BCBL-1 cells following
315 incubation of these cells with soluble Vpr protein at 1, 10, 50, 100, and 200 ng/mL. We
316 found that Vpr was efficiently internalized by BC3 and BCBL-1 cells (Fig. 1E and data not
317 shown).

318 Uninduced PEL cells are latently infected by KSHV, however, they often have low level
319 of spontaneous viral lytic replication (8). To determine the effect of soluble Vpr protein on
320 KSHV lytic replication, we examined extracellular viral genome copy numbers, which
321 reflected the production of viral particles, upon exposure of the uninduced PEL cells to
322 soluble Vpr. As shown in Fig. 2A, the production of viral particles upon exposure of the
323 uninduced PEL cells to soluble Vpr was decreased in a dose-dependent manner. Moreover,
324 the maximum decrease of viral particles was observed when 50 ng/ml soluble Vpr was used
325 (Fig. 2A). Based on the above results and previous studies (36, 50, 51, 53-56), we chose 50
326 ng/ml soluble Vpr for the subsequent experiments. Western blots showed that Vpr not only
327 decreased the levels of KSHV lytic proteins including RTA (ORF50), vIL-6 (ORF-K2) and
328 ORF65 in BC3 cells and BCBL-1 cells incubated with soluble Vpr protein from 6 h to 72 h,
329 but also increased the expression level of latency-associated nuclear antigen (LANA)
330 encoded by ORF73 in BCBL-1 cells (Fig. 2B). Results of RT-qPCR showed that soluble Vpr
331 decreased the expression of KSHV lytic transcripts examined including ORF21, ORF57,
332 ORF59, polyadenylated nuclear (PAN), and ORF-K9 while increased the expression level of
333 LANA transcript (Fig. 2C). Collectively, these results indicated that soluble Vpr was
334 efficiently internalized into PEL cells, and the internalized Vpr likely inhibited the reactivation

335 of KSHV lytic replication program.

336

337 **Internalized Vpr protein activates NF- κ B signaling to inhibit KSHV replication in PEL**
338 **cells**

339 The NF- κ B pathway, which is activated by HIV-1 infection, inhibits KSHV reactivation in
340 BCBL-1 cells (16, 57). The I κ B α acts as the major upstream inhibitor of NF- κ B complex. To
341 determine if Vpr might regulate the NF- κ B pathway, we examined the expression level of
342 I κ B α in BC3 cells and BCBL-1 cells exposed to soluble Vpr for 24, 48 and 72 h. Soluble Vpr
343 not only inhibited the expression of KSHV lytic protein vIL-6 but also repressed the level of
344 I κ B α protein, suggesting Vpr might activate the NF- κ B pathway (Fig. 3A).
345 Immunofluorescence staining showed that more nuclear translocation of p65 was observed
346 in BC3 cells following incubation with soluble Vpr (Fig. 3B). In addition, ELISA-based NF- κ B
347 activity assay demonstrated that the transcriptional activity of NF- κ B p65 in BC3 cells and
348 BCBL-1 cells incubated with soluble Vpr was significantly higher than that of the control
349 cells treated with PBS (Fig. 3C). Moreover, Vpr also increased the NF- κ B luciferase reporter
350 activity in BC3 and BCBL-1 cells (Fig. 3D).

351 To confirm that the activated NF- κ B pathway mediated soluble Vpr inhibition of KSHV
352 lytic replication, BC3 cells and BCBL-1 cells were transduced with lentiviral viruses
353 expressing a constitutively active I κ B α construct, I κ B-DN, to inhibit the NF- κ B pathway, and
354 then incubated with soluble Vpr for 72 h. Expression of I κ B-DN reversed the suppression of
355 vIL-6 by Vpr (Fig. 4A). As expected, the expression of I κ B-DN also reversed the
356 Vpr-induced p65 nuclear translocation (Fig. 4B), p65 binding to the NF- κ B consensus site

357 (Fig. 4C), and the NF- κ B reporter activity (Fig. 4D). In agreement with the inhibition of
358 NF- κ B activity by I κ B-DN, we observed reduced inhibitory effects of Vpr on the production
359 of viral particles and expression of KSHV lytic transcripts (Fig. 4E and 4F). To explore
360 whether the inhibitory effect of soluble Vpr protein on KSHV lytic replication could be
361 neutralized by an anti-Vpr antibody, BC3 and BCBL-1 cells were incubated with soluble Vpr
362 in the absence or presence of an anti-Vpr antibody for 24 and 72 h. As shown in Fig. 4G,
363 Vpr inhibition of KSHV virion production was blocked by treatment with an anti-Vpr antibody
364 but was not affected by the goat IgG antibody control, thus confirming that Vpr inhibition of
365 KSHV lytic replication was directly due to the presence of extracellular Vpr in the
366 conditioned medium. Taken together, these results indicated that internalized Vpr protein
367 activated NF- κ B signaling pathway in PEL cells, which mediated the inhibition of KSHV lytic
368 replication by Vpr.

369

370 **I κ B α 3'UTR is directly targeted by cellular miR-942-5p**

371 We have previously shown that cellular miR-891a-5p mediates Tat and K1 synergistic
372 induction of angiogenesis by targeting I κ B α to activate the NF- κ B pathway (39). To
373 determine if miRNA(s) was involved in Vpr downregulation of I κ B α , we examined the
374 expression profiles of miRNAs by microarray analysis of BC3 cells following incubation with
375 soluble Vpr or PBS control for 72 h. Among hundreds of miRNAs altered by Vpr, six of
376 upregulated miRNAs had putative targeting sites in I κ B α 3'UTR based on the results of
377 miRNA target prediction software, including PITA, RNAhybrid and RNA22 (Fig. 5A). I κ B α
378 3'UTR luciferase reporter assay indicated that five of them suppressed the activity of I κ B α
379 3'UTR reporter (Fig. 5B); however, only cellular miR-942-5p reproducibly inhibited the

380 endogenous I κ B α protein expression in BC3 cells (Fig. 5C), which was chosen for further
381 validation. Indeed, miR-942-5p repressed the activity of I κ B α 3'UTR reporter but not the
382 control reporter pGL3 (Fig. 5D). Incubation with soluble Vpr for 72 h increased the
383 expression level of miR-942-5p in BC3 and BCBL-1 cells (Fig. 5E). miR-942-5p inhibited
384 the I κ B α 3'UTR reporter activity and endogenous I κ B α protein level in BC3 cells in a
385 dose-dependent manner (Figs. 5F and 5G). On the contrary, an inhibitor of miR-942-5p
386 increased the endogenous I κ B α protein level in BC3 cells (Fig. 5H). Based on the
387 bioinformatics predicted miR-942-5p targeting site in the I κ B α 3'UTR, we performed
388 mutagenesis with the I κ B α 3'UTR reporter and miR-942-5p (Fig. 5I). Mutation of the
389 targeting site in the I κ B α 3'UTR reporter abolished the inhibitory effect of miR-942-5p.
390 Similarly, mutation of the miR-942-5p rendered it ineffective in inhibiting the I κ B α 3'UTR
391 reporter activity (Fig. 5J). The mutant miR-942-5p mimic also failed to inhibit the I κ B α
392 protein expression (Fig. 5K). These results demonstrated that I κ B α 3'UTR was directly
393 targeted by the soluble Vpr-upregulated miR-942-5p.

394

395 **miR-942-5p mediates soluble Vpr inhibition of KSHV lytic replication by targeting**
396 **I κ B α to activate the NF- κ B pathway**

397 To examine the role of miR-942-5p in soluble Vpr inhibition of I κ B α and in KSHV lytic
398 replication, we transfected an inhibitor of miR-942-5p or a scramble control into BC3 and
399 BCBL-1 cells followed by incubation with soluble Vpr. Western blot analysis showed that the
400 expression of I κ B α and ORF65 were elevated in Vpr-treated cells transfected with the
401 inhibitor of miR-942-5p compared with cells transfected with the scrambled control (Fig. 6A).
402 Accordingly, the level of NF- κ B p65 nuclear translocation (Fig. 6B) and the NF- κ B reporter

403 activity (Fig. 6C) were reduced in Vpr-treated cells transfected with the miR-942-5p inhibitor.
404 Furthermore, the inhibitory effect of soluble Vpr on the production of viral particles and
405 KSHV lytic transcripts was relieved by the miR-942-5p inhibitor (Figs. 6D and 6E).
406 Consistent with these results, transfection of a synthetic mimic of miR-942-5p inhibited the
407 expression of I κ B α and ORF65 proteins in BC3 cells (Fig. 7A). MiR-942-5p mimic further
408 increased the NF- κ B luciferase reporter activity (Fig. 7B), inhibited the production of viral
409 particles (Fig. 7C) and reduced the expression levels of KSHV lytic transcripts (Fig. 7D)
410 exerted by soluble Vpr. Furthermore, transfection of the miR-942-5p inhibitor alone was
411 sufficient to significantly increase the expression of I κ B α and ORF65 proteins as well as the
412 production of viral particles (Figs. 8A and 8B). In contrast, overexpression of miR-942-5p in
413 BC3 cells and BCBL-1 cells without Vpr protein was sufficient to inhibit the expression of
414 I κ B α and ORF65 proteins as well as the production of viral particles (Figs. 8C and 8D).
415 Collectively, these results indicated that soluble Vpr upregulated cellular miR-942-5p, which
416 then directly targeted I κ B α to activate the NF- κ B pathway and inhibit KSHV lytic replication.

417

418

419

420

421 Discussion

422 Like other herpesviruses, KSHV exhibits a biphasic lifecycle consisting of a reversible
423 latent phase and a transient lytic replication phase. KSHV latent infection evades host
424 immune surveillance and facilitates the establishment of a lifelong persistent infection. As
425 KSHV is a necessary but not sufficient etiological factor for KS, understanding of the

426 mechanisms of KSHV latency and reactivation in the context of cofactors such as HIV-1
427 infection is critical for delineating the pathogenesis of KSHV-associated diseases. Although
428 KS tumor cells are not directly infected by HIV-1, they are exposed to free HIV-1 viral
429 particles and circulating soluble HIV proteins, which may dysregulate KSHV lifecycle.
430 Interestingly, we have previously revealed that Tat produced by HIV-1-infected cells can
431 trigger KSHV reactivation from latency, resulting in the release of progeny virions (21) while
432 HIV-1 Nef delivered in the form of soluble protein or by transfection with an expression
433 plasmid inhibits KSHV replication by regulating cellular miR-1258 (26).

434 Importantly, similar to secreted Tat and Nef proteins, Vpr, an accessory gene product
435 of HIV-1, is detected in the serum and CSF of HIV-positive individuals at a concentration as
436 high as 10 ng/ml (35, 51). Whether the extracellular form of Vpr is secreted from the HIV-1
437 infected cells or derived from the breakdown of infected cells or virus particles remains
438 elusive. However, purified Vpr (synthetic or expressed through baculovirus) has been
439 shown to enter the cells (36, 49-52), suggesting that Vpr may use receptors present on the
440 cell surface for its internalization or may contain signal sequences that enable its entry into
441 cells independent of the receptor pathway. In this study, we have revealed, for the first time,
442 that soluble Vpr can be internalized by B cells *in vitro* and that, similar to HIV-1 Tat and Nef,
443 respectively, the internalized Vpr is functional in a HIV-1 LTR reporter assay and can inhibit
444 the expression of KSHV lytic genes and production of viral particles. The diverse functions
445 of HIV-1 secreted proteins in controlling the balance between KSHV latency and lytic
446 replication might reflect a delicate role of HIV-1 infection in KSHV persistent infection,
447 evasion of host immune response, and induction of KSHV-associated malignancies.

448 The NF- κ B family and the related transcription factors regulate the tumorigenesis of

449 oncogenic viruses, including KSHV (57-59). HIV-1 Vpr has been shown to regulate the
450 NF- κ B activity with controversial subsequences. Numerous studies have shown that
451 virion-derived Vpr and extracellular Vpr can activate the NF- κ B pathway in various cell
452 types and enhance the transcription from the HIV-1 LTR promoter (53, 60-62). The
453 underlying mechanisms may include the interaction with IKK α / β to induce phosphorylation
454 of p65 and p100 (63), and/or the activation of transforming growth factor- β -activated kinase
455 1 (TAK1) to modulate the production of proinflammatory cytokines expression which are
456 beneficial for virus replication (64). It has also been reported that the synthetic Vpr activates
457 NF- κ B pathway and stimulates HIV-1 transcription in U937 and primary macrophages (53).
458 In contrast, Vpr derived from an adenoviral vector exhibits inhibitory effects on the NF- κ B
459 pathway activated by tumor necrosis factor- α (TNF- α) but not lipopolysaccharides (LPS)
460 (65). Indeed, David B. Weiner *et al.* have previously reported that recombinant HIV-1 pNL43
461 Vpr protein diminishes the NF- κ B activity by upregulating I κ B α transcription (66). In spite of
462 conflicting stimulatory and inhibitory effects of Vpr on NF- κ B pathway depending on cellular
463 context or expression manner of Vpr, our findings have identified a novel role of a cellular
464 miRNA in Vpr activation of the NF- κ B pathway in KSHV-infected cells.

465 MiRNAs are a class of small single-stranded noncoding RNAs of approximately 22
466 nucleotides that modulates the expression of a network of mRNAs by binding to imperfect
467 sequences. Dysregulation of miRNA-mediated posttranscriptional regulatory activity
468 appears to critically influence the "latent to lytic" switch in KSHV lifecycle and contribute to
469 KS progression, through either direct targeting of the viral switch protein, RTA (67, 68), or
470 via indirect mechanisms including targeting host factors such as I κ B α , nuclear factor I/B
471 (NFIB), retinoblastoma-like 2 (Rbl2), Bcl-2 associated factor 1 (BCLAF1), and IKK ϵ (44,

472 69-72). For example, we have previously shown that soluble and ectopic expression of
473 HIV-1-encoded Nef protein could suppress the expression of KSHV lytic proteins and the
474 production of viral particles through regulation of cellular miR-1258 that directly targets the
475 3'UTR of KSHV RTA (26).

476 Three cellular miRNAs (miR-126, miR-30e* and miR-196a) target I κ B α 3'UTR, which
477 increase the occurrence of ulcer disease, glioma, and pancreatic cancer, respectively
478 (73-75). miR-K1 encoded by KSHV has also been found to regulate the I κ B α protein level to
479 inhibit viral lytic replication and enhance cell proliferation, survival and cellular
480 transformation (44, 76). Interestingly, we have recently revealed that HIV-1 Tat synergized
481 with KSHV ORF-K1 to increase the expression of miR-891a-5p, which directly targeted
482 I κ B α , leading to enhanced angiogenesis in endothelial cells (39). In this study, cellular
483 miR-942-5p upregulated by HIV-1 Vpr is shown to directly target a seed sequence in the
484 3'UTR of I κ B α and is involved in Vpr inhibition of KSHV lytic replication. A number of KSHV
485 miRNAs also indirectly regulate I κ B α and NF- κ B pathway to promote KSHV-induced cellular
486 transformation and tumorigenesis (76). Therefore, there are complex interactions among
487 miRNAs and I κ B α during NF- κ B activation and subsequent cancer development.
488 Importantly, miR-942 up-regulates matrix metalloproteinase-9 (MMP-9) and vascular
489 endothelial growth factor (VEGF) secretion contributing to endothelial migration and
490 sunitinib resistance in metastatic renal-cell-carcinoma (MRCC) cells (77). Moreover,
491 miR-942 is inversely correlated with the expression of interferon-stimulated gene 12a
492 (ISG12a) and modulates tumor necrosis factor-related apoptosis-inducing ligand (TRAIL)
493 sensitivity in cancer tissues and cells (78). Recently, miR-942 is shown to be upregulated in
494 esophageal squamous cell carcinoma (ESCC) and to promote the stem cell-like traits by

495 inhibiting three negative regulators of the Wnt/ β -catenin pathway including secreted
496 Frizzled-related protein 4 (sFRP4), glycogen synthase kinase 3 β (GSK3 β) and
497 transducin-like enhancer of split 1 (TLE1) (79). In addition, the high expression levels of
498 miR-942 have been detected in nephrotic syndrome patients and lung cancer cases (80,
499 81). Thus, miR-942 is an Onco-miR that might be a potential therapeutic target for some
500 types of cancers.

501 In summary, our results demonstrate that as a soluble protein, internalized HIV-1 Vpr
502 can activate the NF- κ B pathway by upregulating the expression of cellular miR-942-5p to
503 target I κ B α . The Vpr activated NF- κ B pathway promotes viral latency by inhibiting KSHV
504 lytic replication and enhances tumor development. Thus, HIV-1-encoded secreted proteins
505 play essential roles in KSHV lifecycle. Further studies will be needed to better understand
506 the mechanism by which Vpr regulates the expression of miR-942-5p, and the possible
507 involvement of other miRNAs in this process. Due to the significant functions of miRNAs in
508 the pathogenesis of KSHV-related malignancies, miRNA-based gene therapy may be an
509 attractive approach for the treatment of AIDS-KS.

510

511

512

513

514 **Acknowledgements**

515 We are grateful to members from Dr. Lu laboratory for helpful discussion.

516

517 **Author Contributions**

518 Conceived and designed the experiments: C.L. Performed the experiments: Q. Y., C.S., J.
519 Q., W.L., M.H. Provided the reagents: H.L., S.J.G. Analyzed the data: Q.Y., D.Q., J. Z., S. J.
520 G., C.L. Wrote the paper: Q.Y., J. Z., S.J.G., C.L.

521

522 Funding

523 National Natural Science Foundation of China [81361120387, 81371824, 31270199,
524 81401662, 81571984]; NIH [R01CA177377, R01CA132637]; Ph.D. Programs Foundation
525 of Ministry of Education of China [20123234110006]; Natural Science Youth Foundation of
526 Jiangsu Province [BK20140908]

527

528 Competing Interests

529 The authors have declared that no competing interests exist.

530

531

532

533

534 Reference

- 535 1. **Ganem D.** 2010. KSHV and the pathogenesis of Kaposi sarcoma: listening to human biology and
536 medicine. *J Clin Invest* **120**:939-949.
- 537 2. **Mesri EA, Cesarman E, Boshoff C.** 2010. Kaposi's sarcoma and its associated herpesvirus. *Nat Rev*
538 *Cancer* **10**:707-719.
- 539 3. **Casper C.** 2011. The increasing burden of HIV-associated malignancies in resource-limited regions.
540 *Annu Rev Med* **62**:157-170.
- 541 4. **Chang Y, Cesarman E, Pessin MS, Lee F, Culpepper J, Knowles DM, Moore PS.** 1994.
542 Identification of herpesvirus-like DNA sequences in AIDS-associated Kaposi's sarcoma. *Science*
543 **266**:1865-1869.
- 544 5. **Cesarman E, Chang Y, Moore PS, Said JW, Knowles DM.** 1995. Kaposi's sarcoma-associated
545 herpesvirus-like DNA sequences in AIDS-related body-cavity-based lymphomas. *N Engl J Med*

- 546 332:1186-1191.
- 547 6. **Dittmer DP, Damania B.** 2007. KSHV-associated disease in the AIDS patient. *Cancer Treat Res*
- 548 **133**:129-139.
- 549 7. **Davis DA, Rinderknecht AS, Zoetewij JP, Aoki Y, Read-Connole EL, Tosato G, Blauvelt A,**
- 550 **Yarchoan R.** 2001. Hypoxia induces lytic replication of Kaposi sarcoma-associated herpesvirus.
- 551 *Blood* **97**:3244-3250.
- 552 8. **Ye F, Zhou F, Bedolla RG, Jones T, Lei X, Kang T, Guadalupe M, Gao SJ.** 2011. Reactive oxygen
- 553 species hydrogen peroxide mediates Kaposi's sarcoma-associated herpesvirus reactivation from
- 554 latency. *PLoS Pathog* **7**:e1002054.
- 555 9. **Fiorelli V, Gendelman R, Samaniego F, Markham PD, Ensoli B.** 1995. Cytokines from activated T
- 556 cells induce normal endothelial cells to acquire the phenotypic and functional features of
- 557 AIDS-Kaposi's sarcoma spindle cells. *J Clin Invest* **95**:1723-1734.
- 558 10. **Mercader M, Taddeo B, Panella JR, Chandran B, Nickoloff BJ, Foreman KE.** 2000. Induction of
- 559 HHV-8 lytic cycle replication by inflammatory cytokines produced by HIV-1-infected T cells. *Am J*
- 560 *Pathol* **156**:1961-1971.
- 561 11. **Ye F, Lei X, Gao SJ.** 2011. Mechanisms of Kaposi's Sarcoma-Associated Herpesvirus Latency and
- 562 Reactivation. *Adv Virol* **2011**.
- 563 12. **Mesri EA, Feitelson MA, Munger K.** 2014. Human viral oncogenesis: a cancer hallmarks analysis.
- 564 *Cell Host Microbe* **15**:266-282.
- 565 13. **Lu C, Zeng Y, Huang Z, Huang L, Qian C, Tang G, Qin D.** 2005. Human herpesvirus 6 activates lytic
- 566 cycle replication of Kaposi's sarcoma-associated herpesvirus. *Am J Pathol* **166**:173-183.
- 567 14. **Qin D, Zeng Y, Qian C, Huang Z, Lv Z, Cheng L, Yao S, Tang Q, Chen X, Lu C.** 2008. Induction of
- 568 lytic cycle replication of Kaposi's sarcoma-associated herpesvirus by herpes simplex virus type 1:
- 569 involvement of IL-10 and IL-4. *Cell Microbiol* **10**:713-728.
- 570 15. **Varthakavi V, Browning PJ, Spearman P.** 1999. Human immunodeficiency virus replication in a
- 571 primary effusion lymphoma cell line stimulates lytic-phase replication of Kaposi's sarcoma-associated
- 572 herpesvirus. *J Virol* **73**:10329-10338.
- 573 16. **Zhu X, Zhou F, Qin D, Zeng Y, Lv Z, Yao S, Lu C.** 2011. Human immunodeficiency virus type 1
- 574 induces lytic cycle replication of Kaposi's-sarcoma-associated herpesvirus: role of Ras/c-Raf/MEK1/2,
- 575 PI3K/AKT, and NF-kappaB signaling pathways. *J Mol Biol* **410**:1035-1051.
- 576 17. **Vieira J, O'Hearn P, Kimball L, Chandran B, Corey L.** 2001. Activation of Kaposi's
- 577 sarcoma-associated herpesvirus (human herpesvirus 8) lytic replication by human cytomegalovirus. *J*
- 578 *Virol* **75**:1378-1386.
- 579 18. **Morris AK, Valley AW.** 1996. Overview of the management of AIDS-related Kaposi's sarcoma. *Ann*
- 580 *Pharmacother* **30**:1150-1163.
- 581 19. **Chang HC, Samaniego F, Nair BC, Buonaguro L, Ensoli B.** 1997. HIV-1 Tat protein exits from cells
- 582 via a leaderless secretory pathway and binds to extracellular matrix-associated heparan sulfate
- 583 proteoglycans through its basic region. *Aids* **11**:1421-1431.
- 584 20. **Raymond AD, Campbell-Sims TC, Khan M, Lang M, Huang MB, Bond VC, Powell MD.** 2011. HIV
- 585 Type 1 Nef is released from infected cells in CD45(+) microvesicles and is present in the plasma of
- 586 HIV-infected individuals. *AIDS Res Hum Retroviruses* **27**:167-178.
- 587 21. **Zeng Y, Zhang X, Huang Z, Cheng L, Yao S, Qin D, Chen X, Tang Q, Lv Z, Zhang L, Lu C.** 2007.
- 588 Intracellular Tat of human immunodeficiency virus type 1 activates lytic cycle replication of Kaposi's
- 589 sarcoma-associated herpesvirus: role of JAK/STAT signaling. *J Virol* **81**:2401-2417.
- 590 22. **Zhou F, Xue M, Qin D, Zhu X, Wang C, Zhu J, Hao T, Cheng L, Chen X, Bai Z, Feng N, Gao SJ, Lu**

- 591 C. 2013. HIV-1 Tat Promotes Kaposi's Sarcoma-Associated Herpesvirus (KSHV) vIL-6-Induced
592 Angiogenesis and Tumorigenesis by Regulating PI3K/PTEN/AKT/GSK-3 β Signaling Pathway.
593 PLoS One **8**:e53145.
- 594 23. **Guo HG, Pati S, Sadowska M, Charurat M, Reitz M.** 2004. Tumorigenesis by human herpesvirus 8
595 vGPCR is accelerated by human immunodeficiency virus type 1 Tat. J Virol **78**:9336-9342.
- 596 24. **Chen X, Cheng L, Jia X, Zeng Y, Yao S, Lv Z, Qin D, Fang X, Lei Y, Lu C.** 2009. Human
597 immunodeficiency virus type 1 Tat accelerates Kaposi sarcoma-associated herpesvirus Kaposin
598 A-mediated tumorigenesis of transformed fibroblasts in vitro as well as in nude and
599 immunocompetent mice. Neoplasia **11**:1272-1284.
- 600 25. **Yao S, Hu M, Hao T, Li W, Xue X, Xue M, Zhu X, Zhou F, Qin D, Yan Q, Zhu J, Gao SJ, Lu C.** 2015.
601 MiRNA-891a-5p mediates HIV-1 Tat and KSHV Orf-K1 synergistic induction of angiogenesis by
602 activating NF- κ B signaling. Nucleic Acids Res **43**:9362-9378.
- 603 26. **Yan Q, Ma X, Shen C, Cao X, Feng N, Qin D, Zeng Y, Zhu J, Gao SJ, Lu C.** 2014. Inhibition of
604 Kaposi's Sarcoma-Associated Herpesvirus Lytic Replication by HIV-1 Nef and Cellular MicroRNA
605 hsa-miR-1258. J Virol **88**:4987-5000.
- 606 27. **Xue M, Yao S, Hu M, Li W, Hao T, Zhou F, Zhu X, Lu H, Qin D, Yan Q, Zhu J, Gao SJ, Lu C.** 2014.
607 HIV-1 Nef and KSHV oncogene K1 synergistically promote angiogenesis by inducing cellular miR-718
608 to regulate the PTEN/AKT/mTOR signaling pathway. Nucleic Acids Res **42**:9862-9879.
- 609 28. **Zhu X, Guo Y, Yao S, Yan Q, Xue M, Hao T, Zhou F, Zhu J, Qin D, Lu C.** 2014. Synergy between
610 Kaposi's sarcoma-associated herpesvirus (KSHV) vIL-6 and HIV-1 Nef protein in promotion of
611 angiogenesis and oncogenesis: role of the AKT signaling pathway. Oncogene **33**:1986-1996.
- 612 29. **Wong-Staal F, Chanda PK, Ghayeb J.** 1987. Human immunodeficiency virus: the eighth gene.
613 AIDS Res Hum Retroviruses **3**:33-39.
- 614 30. **Heinzinger NK, Bukrinsky MI, Haggerty SA, Ragland AM, Kewalramani V, Lee MA, Gendelman
615 HE, Ratner L, Stevenson M, Emerman M.** 1994. The Vpr protein of human immunodeficiency virus
616 type 1 influences nuclear localization of viral nucleic acids in nondividing host cells. Proc Natl Acad
617 Sci U S A **91**:7311-7315.
- 618 31. **Jowett JB, Planelles V, Poon B, Shah NP, Chen ML, Chen IS.** 1995. The human immunodeficiency
619 virus type 1 vpr gene arrests infected T cells in the G2 + M phase of the cell cycle. J Virol
620 **69**:6304-6313.
- 621 32. **Re F, Braaten D, Franke EK, Luban J.** 1995. Human immunodeficiency virus type 1 Vpr arrests the
622 cell cycle in G2 by inhibiting the activation of p34cdc2-cyclin B. J Virol **69**:6859-6864.
- 623 33. **Cohen EA, Terwilliger EF, Jalinoos Y, Proulx J, Sodroski JG, Haseltine WA.** 1990. Identification of
624 HIV-1 vpr product and function. J Acquir Immune Defic Syndr **3**:11-18.
- 625 34. **Stewart SA, Poon B, Jowett JB, Chen IS.** 1997. Human immunodeficiency virus type 1 Vpr induces
626 apoptosis following cell cycle arrest. J Virol **71**:5579-5592.
- 627 35. **Levy DN, Refaeli Y, MacGregor RR, Weiner DB.** 1994. Serum Vpr regulates productive infection
628 and latency of human immunodeficiency virus type 1. Proc Natl Acad Sci U S A **91**:10873-10877.
- 629 36. **Jones GJ, Barsby NL, Cohen EA, Holden J, Harris K, Dickie P, Jhamandas J, Power C.** 2007.
630 HIV-1 Vpr causes neuronal apoptosis and in vivo neurodegeneration. J Neurosci **27**:3703-3711.
- 631 37. **Hoshino S, Sun B, Konishi M, Shimura M, Segawa T, Hagiwara Y, Koyanagi Y, Iwamoto A,
632 Mimaya J, Terunuma H, Kano S, Ishizaka Y.** 2007. Vpr in plasma of HIV type 1-positive patients is
633 correlated with the HIV type 1 RNA titers. AIDS Res Hum Retroviruses **23**:391-397.
- 634 38. **Xiao Y, Chen G, Richard J, Rougeau N, Li H, Seidah NG, Cohen EA.** 2008. Cell-surface
635 processing of extracellular human immunodeficiency virus type 1 Vpr by proprotein convertases.

- 636 Virology **372**:384-397.
- 637 39. **Yao S, Hu M, Hao T, Li W, Xue X, Xue M, Zhu X, Zhou F, Qin D, Yan Q, Zhu J, Gao SJ, Lu C.** 2015.
- 638 MiRNA-891a-5p mediates HIV-1 Tat and KSHV Orf-K1 synergistic induction of angiogenesis by
- 639 activating NF-kappaB signaling. *Nucleic Acids Res* **43**:9362-9378.
- 640 40. **Tachiwana H, Shimura M, Nakai-Murakami C, Tokunaga K, Takizawa Y, Sata T, Kurumizaka H,**
- 641 **Ishizaka Y.** 2006. HIV-1 Vpr induces DNA double-strand breaks. *Cancer Res* **66**:627-631.
- 642 41. **Ferrucci A, Nonnemacher MR, Wigdahl B.** 2013. Extracellular HIV-1 viral protein R affects
- 643 astrocytic glyceraldehyde 3-phosphate dehydrogenase activity and neuronal survival. *J Neurovirol*
- 644 **19**:239-253.
- 645 42. **Gao SJ, Deng JH, Zhou FC.** 2003. Productive lytic replication of a recombinant Kaposi's
- 646 sarcoma-associated herpesvirus in efficient primary infection of primary human endothelial cells. *J*
- 647 *Virol* **77**:9738-9749.
- 648 43. **Yan Q, Li W, Tang Q, Yao S, Lv Z, Feng N, Ma X, Bai Z, Zeng Y, Qin D, Lu C.** 2013. Cellular
- 649 MicroRNAs 498 and 320d Regulate Herpes Simplex Virus 1 Induction of Kaposi's
- 650 Sarcoma-Associated Herpesvirus Lytic Replication by Targeting RTA. *PLoS One* **8**:e55832.
- 651 44. **Lei X, Bai Z, Ye F, Xie J, Kim CG, Huang Y, Gao SJ.** 2010. Regulation of NF-kappaB inhibitor
- 652 IkappaBalpha and viral replication by a KSHV microRNA. *Nat Cell Biol* **12**:193-199.
- 653 45. **Krishnan HH, Naranatt PP, Smith MS, Zeng L, Bloomer C, Chandran B.** 2004. Concurrent
- 654 expression of latent and a limited number of lytic genes with immune modulation and antiapoptotic
- 655 function by Kaposi's sarcoma-associated herpesvirus early during infection of primary endothelial and
- 656 fibroblast cells and subsequent decline of lytic gene expression. *J Virol* **78**:3601-3620.
- 657 46. **Kim S, Domon-Dell C, Kang J, Chung DH, Freund JN, Evers BM.** 2004. Down-regulation of the
- 658 tumor suppressor PTEN by the tumor necrosis factor-alpha/nuclear factor-kappaB
- 659 (NF-kappaB)-inducing kinase/NF-kappaB pathway is linked to a default IkappaB-alpha autoregulatory
- 660 loop. *J Biol Chem* **279**:4285-4291.
- 661 47. **Tang Q, Qin D, Lv Z, Zhu X, Ma X, Yan Q, Zeng Y, Guo Y, Feng N, Lu C.** 2012. Herpes Simplex
- 662 Virus Type 2 Triggers Reactivation of Kaposi's Sarcoma-Associated Herpesvirus from Latency and
- 663 Collaborates with HIV-1 Tat. *PLoS One* **7**:e31652.
- 664 48. **Wang L, Mukherjee S, Jia F, Narayan O, Zhao LJ.** 1995. Interaction of virion protein Vpr of human
- 665 immunodeficiency virus type 1 with cellular transcription factor Sp1 and trans-activation of viral long
- 666 terminal repeat. *J Biol Chem* **270**:25564-25569.
- 667 49. **Henklein P, Bruns K, Sherman MP, Tessmer U, Licha K, Kopp J, de Noronha CM, Greene WC,**
- 668 **Wray V, Schubert U.** 2000. Functional and structural characterization of synthetic HIV-1 Vpr that
- 669 transduces cells, localizes to the nucleus, and induces G2 cell cycle arrest. *J Biol Chem*
- 670 **275**:32016-32026.
- 671 50. **Sherman MP, Schubert U, Williams SA, de Noronha CM, Kreisberg JF, Henklein P, Greene WC.**
- 672 2002. HIV-1 Vpr displays natural protein-transducing properties: implications for viral pathogenesis.
- 673 *Virology* **302**:95-105.
- 674 51. **Levy DN, Refaeli Y, Weiner DB.** 1995. Extracellular Vpr protein increases cellular permissiveness to
- 675 human immunodeficiency virus replication and reactivates virus from latency. *J Virol* **69**:1243-1252.
- 676 52. **Huang MB, Weeks O, Zhao LJ, Saltarelli M, Bond VC.** 2000. Effects of extracellular human
- 677 immunodeficiency virus type 1 vpr protein in primary rat cortical cell cultures. *J Neurovirol* **6**:202-220.
- 678 53. **Varin A, Decrion AZ, Sabbah E, Quivy V, Sire J, Van Lint C, Roques BP, Aggarwal BB, Herbein**
- 679 **G.** 2005. Synthetic Vpr protein activates activator protein-1, c-Jun N-terminal kinase, and NF-kappaB
- 680 and stimulates HIV-1 transcription in promonocytic cells and primary macrophages. *J Biol Chem*

- 280:42557-42567.
54. **Iijima K, Okudaira N, Tamura M, Doi A, Saito Y, Shimura M, Goto M, Matsunaga A, Kawamura YI, Otsubo T, Dohi T, Hoshino S, Kano S, Hagiwara S, Tanuma J, Gatanaga H, Baba M, Iguchi T, Yanagita M, Oka S, Okamura T, Ishizaka Y.** 2013. Viral protein R of human immunodeficiency virus type-1 induces retrotransposition of long interspersed element-1. *Retrovirology* **10**:83.
 55. **Richard J, Pham TN, Ishizaka Y, Cohen EA.** 2013. Viral protein R upregulates expression of ULBP2 on uninfected bystander cells during HIV-1 infection of primary CD4+ T lymphocytes. *Virology* **443**:248-256.
 56. **Rom I, Deshmane SL, Mukerjee R, Khalili K, Amini S, Sawaya BE.** 2009. HIV-1 Vpr deregulates calcium secretion in neural cells. *Brain Res* **1275**:81-86.
 57. **Grossmann C, Ganem D.** 2008. Effects of NFkappaB activation on KSHV latency and lytic reactivation are complex and context-dependent. *Virology* **375**:94-102.
 58. **Izumiya Y, Izumiya C, Hsia D, Ellison TJ, Luciw PA, Kung HJ.** 2009. NF-kappaB serves as a cellular sensor of Kaposi's sarcoma-associated herpesvirus latency and negatively regulates K-Rta by antagonizing the RBP-Jkappa coactivator. *J Virol* **83**:4435-4446.
 59. **Schwarz M, Murphy PM.** 2001. Kaposi's sarcoma-associated herpesvirus G protein-coupled receptor constitutively activates NF-kappa B and induces proinflammatory cytokine and chemokine production via a C-terminal signaling determinant. *J Immunol* **167**:505-513.
 60. **Subbramanian RA, Kessous-Elbaz A, Lodge R, Forget J, Yao XJ, Bergeron D, Cohen EA.** 1998. Human immunodeficiency virus type 1 Vpr is a positive regulator of viral transcription and infectivity in primary human macrophages. *J Exp Med* **187**:1103-1111.
 61. **Roux P, Alfieri C, Hrimech M, Cohen EA, Tanner JE.** 2000. Activation of transcription factors NF-kappaB and NF-IL-6 by human immunodeficiency virus type 1 protein R (Vpr) induces interleukin-8 expression. *J Virol* **74**:4658-4665.
 62. **Hoshino S, Konishi M, Mori M, Shimura M, Nishitani C, Kuroki Y, Koyanagi Y, Kano S, Itabe H, Ishizaka Y.** 2010. HIV-1 Vpr induces TLR4/MyD88-mediated IL-6 production and reactivates viral production from latency. *J Leukoc Biol* **87**:1133-1143.
 63. **Liu R, Tan J, Lin Y, Jia R, Yang W, Liang C, Geng Y, Qiao W.** 2013. HIV-1 Vpr activates both canonical and noncanonical NF-kappaB pathway by enhancing the phosphorylation of IKKalpha/beta. *Virology* **439**:47-56.
 64. **Liu R, Lin Y, Jia R, Geng Y, Liang C, Tan J, Qiao W.** 2014. HIV-1 Vpr stimulates NF-kappaB and AP-1 signaling by activating TAK1. *Retrovirology* **11**:45.
 65. **Kogan M, Deshmane S, Sawaya BE, Gracely EJ, Khalili K, Rappaport J.** 2013. Inhibition of NF-kappaB activity by HIV-1 Vpr is dependent on Vpr binding protein. *J Cell Physiol* **228**:781-790.
 66. **Ayyavoo V, Mahboubi A, Mahalingam S, Ramalingam R, Kudchodkar S, Williams WV, Green DR, Weiner DB.** 1997. HIV-1 Vpr suppresses immune activation and apoptosis through regulation of nuclear factor kappa B. *Nat Med* **3**:1117-1123.
 67. **Lin X, Liang D, He Z, Deng Q, Robertson ES, Lan K.** 2011. miR-K12-7-5p encoded by Kaposi's sarcoma-associated herpesvirus stabilizes the latent state by targeting viral ORF50/RTA. *PLoS One* **6**:e16224.
 68. **Bellare P, Ganem D.** 2009. Regulation of KSHV lytic switch protein expression by a virus-encoded microRNA: an evolutionary adaptation that fine-tunes lytic reactivation. *Cell Host Microbe* **6**:570-575.
 69. **Lu CC, Li Z, Chu CY, Feng J, Feng J, Sun R, Rana TM.** 2010. MicroRNAs encoded by Kaposi's sarcoma-associated herpesvirus regulate viral life cycle. *EMBO Rep* **11**:784-790.
 70. **Lu F, Stedman W, Yousef M, Renne R, Lieberman PM.** 2010. Epigenetic regulation of Kaposi's

- 726 sarcoma-associated herpesvirus latency by virus-encoded microRNAs that target Rta and the cellular
727 Rbl2-DNMT pathway. *J Virol* **84**:2697-2706.
- 728 71. **Liang D, Gao Y, Lin X, He Z, Zhao Q, Deng Q, Lan K.** 2011. A human herpesvirus miRNA attenuates
729 interferon signaling and contributes to maintenance of viral latency by targeting IKKepsilon. *Cell Res*
730 **21**:793-806.
- 731 72. **Ziegelbauer JM, Sullivan CS, Ganem D.** 2009. Tandem array-based expression screens identify
732 host mRNA targets of virus-encoded microRNAs. *Nat Genet* **41**:130-134.
- 733 73. **Feng X, Wang H, Ye S, Guan J, Tan W, Cheng S, Wei G, Wu W, Wu F, Zhou Y.** 2012. Up-regulation
734 of microRNA-126 may contribute to pathogenesis of ulcerative colitis via regulating NF-kappaB
735 inhibitor IkappaBalpha. *PLoS One* **7**:e52782.
- 736 74. **Jiang L, Lin C, Song L, Wu J, Chen B, Ying Z, Fang L, Yan X, He M, Li J, Li M.** 2012.
737 MicroRNA-30e* promotes human glioma cell invasiveness in an orthotopic xenotransplantation model
738 by disrupting the NF-kappaB/IkappaBalpha negative feedback loop. *J Clin Invest* **122**:33-47.
- 739 75. **Huang F, Tang J, Zhuang X, Zhuang Y, Cheng W, Chen W, Yao H, Zhang S.** 2014. MiR-196a
740 promotes pancreatic cancer progression by targeting nuclear factor kappa-B-inhibitor alpha. *PLoS*
741 *One* **9**:e87897.
- 742 76. **Moody R, Zhu Y, Huang Y, Cui X, Jones T, Bedolla R, Lei X, Bai Z, Gao SJ.** 2013. KSHV
743 MicroRNAs Mediate Cellular Transformation and Tumorigenesis by Redundantly Targeting Cell
744 Growth and Survival Pathways. *PLoS Pathog* **9**:e1003857.
- 745 77. **Prior C, Perez-Gracia JL, Garcia-Donas J, Rodriguez-Antona C, Guruceaga E, Esteban E,**
746 **Suarez C, Castellano D, del Alba AG, Lozano MD, Carles J, Climent MA, Arranz JA, Gallardo E,**
747 **Puente J, Bellmunt J, Gurrpide A, Lopez-Picazo JM, Hernandez AG, Mellado B, Martinez E,**
748 **Moreno F, Font A, Calvo A.** 2014. Identification of tissue microRNAs predictive of sunitinib activity in
749 patients with metastatic renal cell carcinoma. *PLoS One* **9**:e86263.
- 750 78. **Liu N, Zuo C, Wang X, Chen T, Yang D, Wang J, Zhu H.** 2014. miR-942 decreases TRAIL-induced
751 apoptosis through ISG12a downregulation and is regulated by AKT. *Oncotarget* **5**:4959-4971.
- 752 79. **Ge C, Wu S, Wang W, Liu Z, Zhang J, Wang Z, Li R, Zhang Z, Li Z, Dong S, Wang Y, Xue Y, Yang**
753 **J, Tan Q, Wang Z, Song X.** 2015. miR-942 promotes cancer stem cell-like traits in esophageal
754 squamous cell carcinoma through activation of Wnt/beta-catenin signalling pathway. *Oncotarget*
755 **6**:10964-10977.
- 756 80. **Teng J, Sun F, Yu PF, Li JX, Yuan D, Chang J, Lin SH.** 2015. Differential microRNA expression in
757 the serum of patients with nephrotic syndrome and clinical correlation analysis. *Int J Clin Exp Pathol*
758 **8**:7282-7286.
- 759 81. **Patnaik SK, Yendamuri S, Kannisto E, Kucharczuk JC, Singhal S, Vachani A.** 2012. MicroRNA
760 expression profiles of whole blood in lung adenocarcinoma. *PLoS One* **7**:e46045.
- 761
- 762
- 763
- 764
- 765
- 766
- 767

768 **Figure Legends**

769 **Figure 1. Soluble Vpr is internalized by PEL cells but does not induce apoptosis.**

770 **(A).** Purified Vpr protein was stained with Coomassie Brilliant Blue R-250. Lane 1, Purified
771 soluble Vpr protein. Lane 2, molecular weight marker. KD, kilodalton.

772 **(B).** Effect of soluble Vpr on HIV-1 LTR transactivation detected by luciferase reporter assay
773 in 293T cells transfected with a HIV-1 LTR luciferase reporter or a pGL3 basic construct in
774 the absence (**PBS**) or presence of soluble Vpr at 50, 100 and 200 ng/mL, respectively. Data
775 represent mean \pm SEM from three independent experiments ($n = 3$), each with four
776 technical replicates.

777 **(C).** Effect of soluble Vpr on apoptosis in BC3 cells. BC3 cells were treated with Vpr at 0, 1,
778 10, 100, 200 and 500 ng/mL for 24 h and examined for apoptosis. x and y axes indicated
779 annexin V (AV) and propidium iodide (PI) staining intensities, respectively.

780 **(D).** Quantification of early, late, and total apoptotic cells in BC3 cells treated with Vpr as
781 described in **(C)**.

782 **(E).** Confocal microscopy of BC3 cells and BCBL-1 cells incubated with 50 ng/ml soluble
783 Vpr (tagged with 6XHis) for 24 h and then stained for KSHV LANA (green) and Vpr (red)
784 with an anti-LANA MAb and an anti-His MAb, respectively. Nuclei were stained with DAPI
785 (blue).

786

787 **Figure 2. Soluble Vpr inhibits KSHV lytic replication in PEL cells.**

788 **(A).** Effect of soluble Vpr on the production of KSHV virions. Supernatants from BC3 cells
789 and BCBL-1 cells incubated with PBS or 0, 1, 10, 50, 100, and 200 ng/ml soluble Vpr for 24
790 h were treated with DNase to eliminate unspecific attachment of DNA. Virion DNA was

791 extracted and quantified by real-time DNA-PCR. The viral copy number was normalized to
792 the PBS group as control. Results shown are a representative experiment of three
793 independent experiments with similar results. Each experiment contains four technical
794 replicates. * $P < 0.05$ and ** $P < 0.01$ by Student's *t* test. *n.s.*, not significant.

795 **(B).** Effect of soluble Vpr on the expression of KSHV lytic proteins. Western blot was
796 performed to detect the expression of KSHV lytic proteins RTA, ORF65 and vIL-6, and
797 latent protein LANA in BC3 or BCBL-1 cells incubated with PBS or 50 ng/ml soluble Vpr for
798 6, 24, 48 and 72 h. The relative intensities of the bands were quantified and normalized to
799 house-keeping protein β -tubulin. The values are labeled under the protein bands. The
800 relative values of proteins in the **PBS** group was set as "1" for comparison.

801 **(C).** Effect of soluble Vpr on the expression of KSHV mRNAs. RT-qPCRs were performed to
802 detect the expression of KSHV lytic transcripts ORF21, ORF57, ORF59, PAN and ORF-K9,
803 and latent transcript LANA in BC3 cells (left panel) and BCBL-1 cells (right panel) treated as
804 described in **(B)**. Results shown are from a representative experiment of three independent
805 experiments with similar results, each experiment containing four technical replicates.

806

807 **Figure 3. Soluble Vpr activates the NF- κ B signaling pathway in PEL cells.**

808 **(A).** Effect of soluble Vpr on the expression of $\text{I}\kappa\text{B}\alpha$ and KSHV lytic protein vIL-6 in PEL cells.
809 Western blot was performed to detect the expression of $\text{I}\kappa\text{B}\alpha$ and KSHV vIL-6 in BC3 cells
810 and BCBL-1 cells incubated with PBS or soluble Vpr for 24, 48 and 72 h.

811 **(B).** Effect of soluble Vpr on the expression and nuclear translocation of NF- κ B p65 in BC3
812 cells observed by confocal microscopy. BC3 cells were incubated with PBS or soluble Vpr
813 for 72 h and then stained for NF- κ B p65 (red) and nuclei (blue) with an anti-p65 MAb and

814 DAPI, respectively.

815 **(C).** Effect of soluble Vpr on NF- κ B p65-DNA binding activity detected by ELISA in PEL cells.

816 Nuclear proteins extracted from BC3 cells and BCBL-1 cells incubated with PBS or soluble

817 Vpr for 72 h were examined in ELISA. Competitive oligonucleotide (**Comp.**) was used as a

818 negative control. Data represent mean \pm SEM determined from three independent

819 experiments (n = 3), each with three technical replicates. *** $P < 0.001$ by Student's t test

820 versus the **PBS** group, while ^{##} $P < 0.01$ and ^{###} $P < 0.001$ by Student's t test versus the

821 **Soluble Vpr** group, respectively.

822 **(D).** Effect of soluble Vpr on NF- κ B activity detected by luciferase reporter assay in PEL

823 cells treated as described in **(C)**. Data represent mean \pm SEM determined from three

824 independent experiments (n = 3), each with four technical replicates. * $P < 0.05$ and ** $P <$

825 0.01 by Student's t test.

826

827 **Figure 4. The NF- κ B signaling pathway mediates soluble Vpr inhibition of in KSHV**

828 **lytic replication.**

829 **(A).** Effect of lentiviral I κ B α -DN transduction on Vpr inhibition of KSHV lytic protein vIL-6 in

830 PEL cells. Western blot was performed to detect the expression of I κ B α and KSHV vIL-6 in

831 BC3 cells and BCBL-1 cells incubated with PBS (**PBS**) or soluble Vpr (**soluble Vpr**) and

832 transduced with lentiviral I κ B α -DN (**I κ B α -DN**) or the empty control (**pCDH**) for 72 h.

833 **(B).** Effect of lentiviral I κ B α -DN transduction on the expression and nuclear translocation of

834 NF- κ B p65 in Vpr treated BC3 cells observed by confocal microscopy. BC3 cells treated as

835 described in **(A)** were stained for NF- κ B p65 (red) and nuclei (blue) with anti-p65 MAb and

836 DAPI, respectively.

837 **(C).** Effect of lentiviral I κ B α -DN transduction on NF- κ B p65-DNA binding activity in Vpr
838 treated PEL cells detected by ELISA. Nuclear proteins extracted from BC3 cells and
839 BCBL-1 cells treated as described in **(A)** were examined by ELISA. Data represent mean \pm
840 SEM determined from three independent experiments ($n = 3$), each with three technical
841 replicates. ** $P < 0.01$ and *** $P < 0.001$ by Student's t test versus the **PBS + pCDH** group,
842 ## $P < 0.01$ and ### $P < 0.001$ by Student's t test versus the **Soluble Vpr + pCDH** group, and
843 && $P < 0.01$ by Student's t test versus the **PBS + pCDH** group, respectively.

844 **(D).** Effect of lentiviral I κ B α -DN transduction on NF- κ B activity detected by luciferase
845 reporter assay in PEL cells treated as described in **(A)**. Data represent mean \pm SEM
846 determined from three independent experiments ($n = 3$), each with four technical replicates.
847 ** $P < 0.01$ and ## $P < 0.01$ by Student's t test versus the **PBS + pCDH** group and the
848 **Soluble Vpr + pCDH** group, respectively.

849 **(E).** Effect of lentiviral I κ B α -DN transduction on the production of KSHV virions in Vpr
850 treated PEL cells. Supernatants from BC3 cells and BCBL-1 cells treated as described in **(A)**
851 for 24, 48 and 72 h were extracted for virion DNA quantification by real-time DNA-PCR.
852 Results shown are a representative experiment of three independent experiments with
853 similar results, each with four technical replicates. * $P < 0.05$, ** $P < 0.01$ and *** $P < 0.001$
854 by Student's t test versus the **PBS + pCDH** group, while ## $P < 0.01$ and ### $P < 0.001$ by
855 Student's t test versus the **Soluble Vpr + pCDH** group, respectively.

856 **(F).** Effect of lentiviral I κ B α -DN transduction on the expression of KSHV lytic mRNAs in Vpr
857 treated PEL cells. RT-qPCRs were performed to detect the expression of KSHV lytic
858 transcripts ORF21, ORF57, ORF59, PAN and ORF-K9 in BC3 cells treated as described in
859 **(E)**. Results shown are a representative experiment of three independent experiments with

860 similar results, each with four technical replicates. * $P < 0.05$ and ** $P < 0.01$ by Student's t
861 test versus the **PBS + pCDH** group, while # $P < 0.05$, ## $P < 0.01$ and ### $P < 0.001$ by
862 Student's t test versus the **Soluble Vpr + pCDH** group, respectively.

863 **(G).** Effect of an anti-Vpr antibody on soluble Vpr inhibition of KSHV virion production in
864 BC-3 and BCBL-1 cells incubated with PBS or soluble Vpr in the presence of goat IgG
865 (**Contr. IgG**) or an anti-Vpr antibody (**pAb-Vpr**), respectively. Supernatants from BC3 cells
866 and BCBL-1 cells treated for 24 and 72 h were extracted for virion DNA quantification by
867 real-time DNA-PCR. Results shown are a representative experiment of three independent
868 experiments with similar results, each with four technical replicates. ** $P < 0.01$ and *** $P <$
869 0.001 by Student's t test versus the **PBS + Contr. IgG** group, while ## $P < 0.01$ and ### $P <$
870 0.001 by Student's t test versus the **Soluble Vpr + Contr. IgG** group, respectively.

871

872 **Figure 5. Identification of miR-942-5p that targets I κ B α 3'UTR.**

873 **(A).** Heat map representation of six microRNAs differentially induced in BC3 cells incubated
874 with PBS (**PBS**) or soluble Vpr (**sVpr**) for 72 h. The expression levels of miRNAs were
875 examined with miRNA microarrays. The experiments were performed with two technical
876 replicates and data represented as means. The color scale from green to red represents
877 low to high expression intensity of miRNAs.

878 **(B).** Verification of six microRNAs identified by miRNA microarray screen by luciferase
879 reporter assay. Mimics of miRNAs (10 nM) as predicted in **(A)** or miRNA negative control
880 (**Neg. Ctrl.**) were co-transfected with pGL3-I κ B α 3'UTR luciferase reporter into HEK293T
881 cells for luciferase reporter assay. Data represent the mean \pm SEM from three independent
882 experiments (n = 3), each with three technical replicates. * $P < 0.05$ and ** $P < 0.01$ by

883 Student's t test; *n.s.*, not significant.

884 **(C).** Effect of six microRNAs identified by miRNA microarray screen on the expression of
885 endogenous I κ B α in BC3 cells transfected with mimics of miRNAs (20 nM) as predicted in
886 **(A)** or miRNA negative control (**Neg. Ctrl.**) for 24 h.

887 **(D).** Effect of miR-942-5p on the reporter activity of the pGL-3-I κ B α 3'UTR and the control
888 reporter pGL3-Control. HEK293T cells were transfected with miR-942-5p (**miR-942-5p**)
889 mimics (10 nM) or miRNA negative control (**Neg. Ctrl.**) along with pGL3-Control or pGL-3-
890 I κ B α 3'UTR reporter plasmid for 24 h. Data represent the mean \pm SEM from three
891 independent experiments (*n* = 3), each with four technical replicates. * *P* < 0.05 by
892 Student's t test versus the **Neg. Ctrl.** group. *n.s.*, not significant.

893 **(E).** Expression of miR-942-5p detected by RT-qPCR in BC3 cells and BCBL-1 cells
894 incubated with PBS or soluble Vpr for 24 h. Data represent the mean \pm SEM from three
895 independent experiments (*n* = 3), each with four technical replicates. * *P* < 0.05 by Student's
896 t test versus the **PBS** group.

897 **(F).** Dose-dependent luciferase reporter assay in HEK293T cells transfected with
898 miR-942-5p mimics (10, 20 and 50 nM) or a negative control (**Neg. Ctrl.**) along with
899 pGL-3-I κ B α 3'UTR reporter plasmid for 24 h. Data represent the mean \pm SEM from three
900 independent experiments (*n* = 3), each with three technical replicates. * *P* < 0.05, ** *P* <
901 0.01 and *** *P* < 0.001 by Student's t test versus the **Neg. Ctrl.** group.

902 **(G).** Dose-dependent Western blot for endogenous I κ B α in BC3 cells transfected with
903 miR-942-5p mimics (10 and 20 nM) or a negative control (**Neg. Ctrl.**) for 24 h.

904 **(H).** Dose-dependent Western blot for endogenous I κ B α in BC3 cells transfected with
905 miR-942-5p inhibitor (10 and 20 nM) or a negative control (**Scr. Ctrl.**) for 24 h.

906 **(I).** Schematic illustration of the putative seed sequences of miR-942-5p target in the I κ B α
907 3'UTR. Binding sites are marked in red, while mutated nucleotides are marked in blue.

908 **(J).** Effect of seed mutation in miR-942-5p or the putative miR-942-5p binding site in the
909 I κ B α 3'UTR on the reporter activity. I κ B α 3'UTR wild type (WT I κ B α) was co-transfected with
910 miRNA mimic negative control (**Neg. Ctrl.**), natural (**miR-942**) or mutant miR-942-5p (**mut**
911 **miR-942**) into HEK293T cells for 24 h, while mutant I κ B α 3'UTR construct (**mut I κ B α**) was
912 also co-transfected with miRNA mimic negative control (**Neg. Ctrl.**), natural (**miR-942**) or
913 mutant miR-942-5p (**mut miR-942**). Data represent the mean \pm SEM from three
914 independent experiments ($n = 3$), each with four technical replicates. * $P < 0.05$ by
915 Student's t-test versus the Neg. Ctrl. plus WT I κ B α group. *n.s.*, not significant.

916 **(K).** Effect of natural and mutant miR-942-5p on the expression of endogenous I κ B α in BC3
917 cells transfected with miR-891a-5p mimics (20 nM), miR-891a-5p mutant and a negative
918 control (**Neg. Ctrl.**) for 24 h.

919

920 **Figure 6. Inhibition of miR-942-5p inactivates the NF- κ B signaling pathway and**
921 **disrupts KSHV latency in PEL cells.**

922 **(A).** Effect of the miR-942-5p inhibitor on the expression of I κ B α and KSHV lytic protein
923 ORF65 in Vpr treated PEL cells. Western blot was performed to detect the expression of
924 I κ B α and KSHV ORF65 in BC3 cells and BCBL-1 cells incubated with PBS (**PBS**) or soluble
925 Vpr (**Soluble Vpr**) and transfected with miR-942-5p inhibitor (**miR-942-5p inhibitor**) or a
926 negative control (**Scr. Ctrl.**) for 72 h. The relative values of proteins in the PBS plus Scr.
927 Ctrl. group was set as "1" for comparison.

928 **(B).** Effect of the miR-942-5p inhibitor on the expression and nuclear translocation of NF- κ B

929 p65 in Vpr-treated PEL cells observed by confocal microscopy. BC3 cells treated as
930 described in (A) were stained for NF- κ B p65 (red) and nuclei (blue) with an anti-p65 MAb
931 and DAPI, respectively.

932 (C). Effect of the miR-942-5p inhibitor on NF- κ B activity detected by luciferase reporter
933 assay in PEL cells treated as described in (A). Data represent mean \pm SEM determined
934 from three independent experiments ($n = 3$), each with four technical replicates. ** $P < 0.01$
935 by Student's t test versus the **PBS + Scr. Ctrl.** group, while # $P < 0.05$ and ## $P < 0.01$ by
936 Student's t test versus the **sVpr + Scr. Ctrl.** group, respectively.

937 (D). Effect of the miR-942-5p inhibitor on the production of KSHV virions in Vpr-treated PEL
938 cells. Supernatants from BC3 cells and BCBL-1 cells treated as described in (A) for 24, 48
939 and 72 h were extracted for virion DNA quantification by real-time DNA-PCR. Results
940 shown are a representative experiment of three independent experiments with similar
941 results, each with four technical replicates. ** $P < 0.01$ and *** $P < 0.001$ by Student's t test
942 versus the **PBS + Scr. Ctrl.** group, while # $P < 0.05$, ## $P < 0.01$ and ### $P < 0.001$ by
943 Student's t test versus the **sVpr + Scr. Ctrl.** group, respectively.

944 (E). Effect of the miR-942-5p inhibitor on the expression of KSHV lytic mRNAs in
945 Vpr-treated PEL cells. RT-qPCRs were performed to detect the expression of KSHV lytic
946 transcripts, ORF21, ORF57, ORF59, PAN and K9 in BC3 cells treated as described in (D).
947 Results shown are a representative experiment of three independent experiments with
948 similar results, each with four technical replicates. * $P < 0.05$ and ** $P < 0.01$ by Student's t
949 test versus the **PBS + Scr. Ctrl.** group, while # $P < 0.05$, ## $P < 0.01$ and ### $P < 0.001$ by
950 Student's t test versus the **sVpr + Scr. Ctrl.** group, respectively.

951

952 **Figure 7. Overexpression of miR-942-5p activates the NF- κ B signaling pathway and**
953 **inhibits KSHV lytic replication in PEL cells.**

954 **(A).** Effect of miR-942-5p mimic on the expression of I κ B α and KSHV lytic protein ORF65 in
955 Vpr-treated PEL cells. Western blot was performed to detect the expression of I κ B α and
956 KSHV ORF65 in BC3 cells and BCBL-1 cells incubated with PBS (**PBS**) or soluble Vpr
957 (**Soluble Vpr**) and transfected with miR-942-5p mimic (**miR-942-5p mimic**) or a negative
958 control (**Neg. Ctrl.**) for 72 h. The relative values of proteins in the PBS plus Neg. Ctrl. group
959 was set as "1" for comparison.

960 **(B).** Effect of miR-942-5p mimic on NF- κ B activity detected by luciferase reporter assay in
961 PEL cells treated as described in **(A)**. Data represent mean \pm SEM determined from three
962 independent experiments (n = 3), each with four technical replicates. ** $P < 0.01$ and *** $P <$
963 0.001 by Student's t test versus the **PBS + Neg. Ctrl.** group, while # $P < 0.05$ by Student's t
964 test versus the **sVpr + Neg. Ctrl.** group, respectively.

965 **(C).** Effect of miR-942-5p mimic on the production of KSHV virions in Vpr-treated PEL cells.
966 Supernatants from BC3 cells and BCBL-1 cells treated as described in **(A)** for 24, 48 and 72
967 h were extracted for virion DNA quantification by real-time DNA-PCR. Results shown are a
968 representative experiment of three independent experiments with similar results, each with
969 four technical replicates. ** $P < 0.01$ and *** $P < 0.001$ by Student's t test versus the **PBS +**
970 **Neg. Ctrl.** group, while # $P < 0.05$ by Student's t test versus the **sVpr + Neg. Ctrl.** group,
971 respectively.

972 **(D).** Effect of miR-942-5p mimic on the expression of KSHV lytic mRNAs in Vpr-treated PEL
973 cells. RT-qPCRs were performed to detect the expression of KSHV lytic transcripts ORF21,
974 ORF57, ORF59, PAN and ORF-K9 in BC3 cells treated as described in **(C)**. Results shown

975 are a representative experiment of three independent experiments with similar results, each
976 with four technical replicates. * $P < 0.05$ and ** $P < 0.01$ by Student's t test versus the **PBS**
977 **+ Neg. Ctrl.** group, while # $P < 0.05$ and ## $P < 0.01$ by Student's t test versus the **sVpr +**
978 **Neg. Ctrl.** group, respectively.

979

980 **Figure 8. MiR-942-5p inhibits KSHV lytic replication by targeting I κ B α .**

981 **(A).** Effect of the miR-942-5p inhibitor on the expression of I κ B α and KSHV lytic protein
982 ORF65 in PEL cells. Western blot was performed to detect the expression of I κ B α and
983 KSHV ORF65 in BC3 cells and BCBL-1 cells transfected with miR-942-5p inhibitor
984 **(miR-942-5p inhibitor)** or a negative control (**Scr. Ctrl.**) for 72 h. The relative values of
985 proteins in the **Scr. Ctrl.** group was set as "1" for comparison.

986 **(B).** Effect of the miR-942-5p inhibitor on the production of KSHV virions in PEL cells.
987 Supernatants from BC3 cells and BCBL-1 cells treated as described in **(A)** for 24 and 72 h
988 were extracted for virion DNA quantification by real-time DNA-PCR. Results shown are a
989 representative experiment of three independent experiments with similar results, each with
990 four technical replicates. ** $P < 0.01$ and *** $P < 0.001$ by Student's t test versus the **Scr.**
991 **Ctrl.** group.

992 **(C).** Effect of miR-942-5p mimic on the expression of I κ B α and KSHV lytic protein ORF65 in
993 PEL cells. Western blot was performed to detect the expression of I κ B α and KSHV ORF65
994 in BC3 cells and BCBL-1 cells transfected with miR-942-5p mimic **(miR-942-5p mimic)** or a
995 negative control (**Neg. Ctrl.**) for 72 h. The relative values of proteins in the **Neg. Ctrl.** group
996 was set as "1" for comparison.

997 **(D).** Effect of miR-942-5p mimic on the production of KSHV virions in PEL cells.

998 Supernatants from BC3 cells and BCBL-1 cells treated as described in (C) for 24 and 72 h
999 were extracted for virion DNA quantification by real-time DNA-PCR. Results shown are a
1000 representative experiment of three independent experiments with similar results, each with
1001 four technical replicates. * $P < 0.05$, ** $P < 0.01$ and *** $P < 0.001$ by Student's t test versus
1002 the **Neg. Ctrl.** group.

1003

1004

1005

1006

1007

1008

1009

1010

1011

1012

1013

1014

1015

1016

1017

1018

1019

1020

1021

1022 **Table 1. Primers for RT-qPCR detection of KSHV genes**

Gene	Primer
KSHV ORF21	F, 5'- CGT AGC CGA CGC GGA TAA -3'
	R, 5'- TGC CTG TAG ATT TCG GTC CAC -3'
KSHV ORF57	F, 5'- TGG CGA GGT CAA GCT TAA CTT C -3'
	R, 5'- CCC CTG GCC TGT AGT ATT CCA -3'
KSHV ORF59	F, 5'- TTG GCA CTC CAA CGA AAT ATT AGA A -3'
	R, 5'- CGG GAA CCT TTT GCG AAG A -3'
KSHV PAN	F, 5'- GCC GCT TCT GGT TTT CAT TG -3'
	R, 5'- TTG CCA AAA GCG ACG CA -3'
KSHV K9	F, 5'- GTC TCT GCG CCA TTC AAA AC -3'
	R, 5'- CCG GAC ACG ACA ACT AAG AA -3'
KSHV LANA	F, 5'- CCG AGG ACG AAA TGG AAG TG -3'
	R, 5'- GGT GAT GTT CTG AGT ACA TAG CGG -3'
β-actin	F, 5'- TTG CCG ACA GGA TGC AGA AGG A -3'
	R, 5'- AGG TGG ACA GCG AGG CCA GGA T -3'

1023 F, forward; R, reverse.

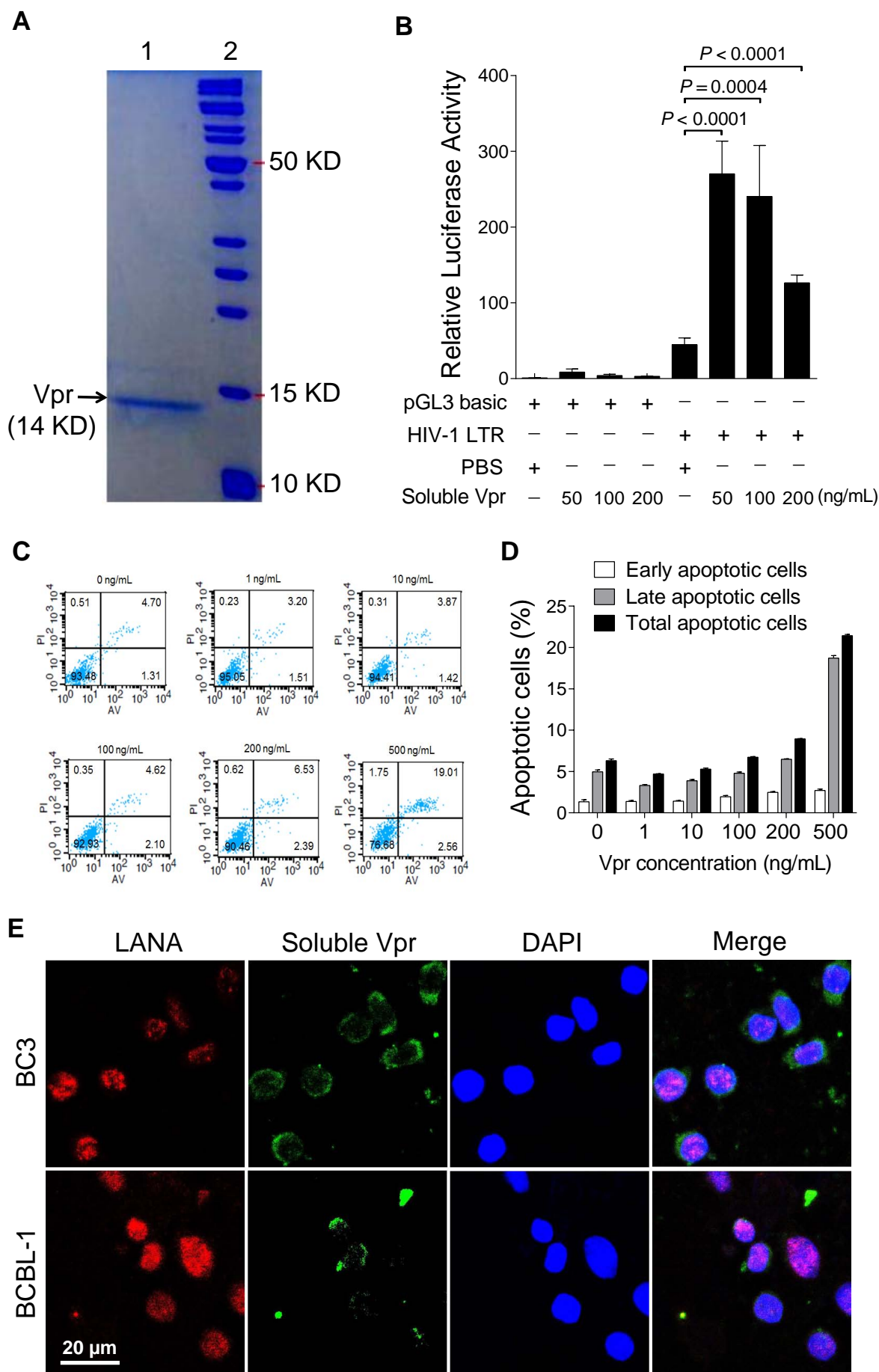


Figure 1

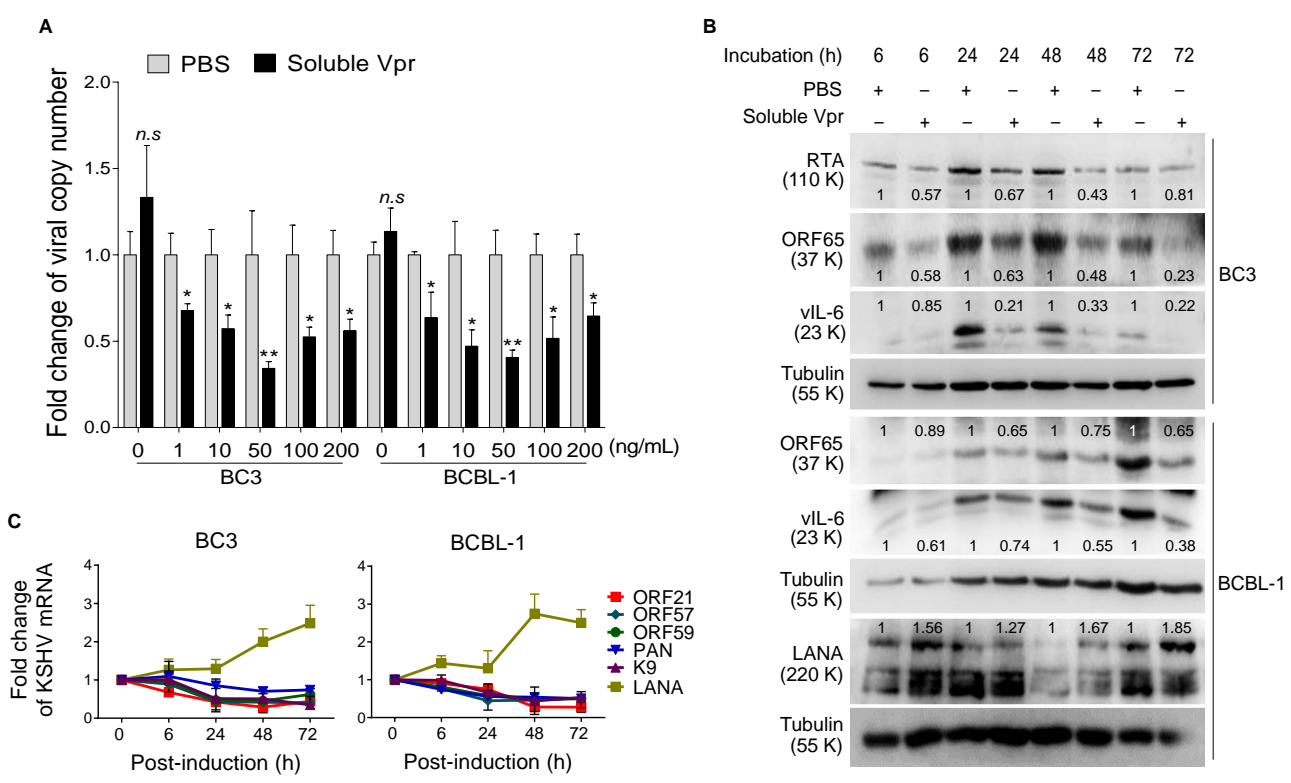


Figure 2

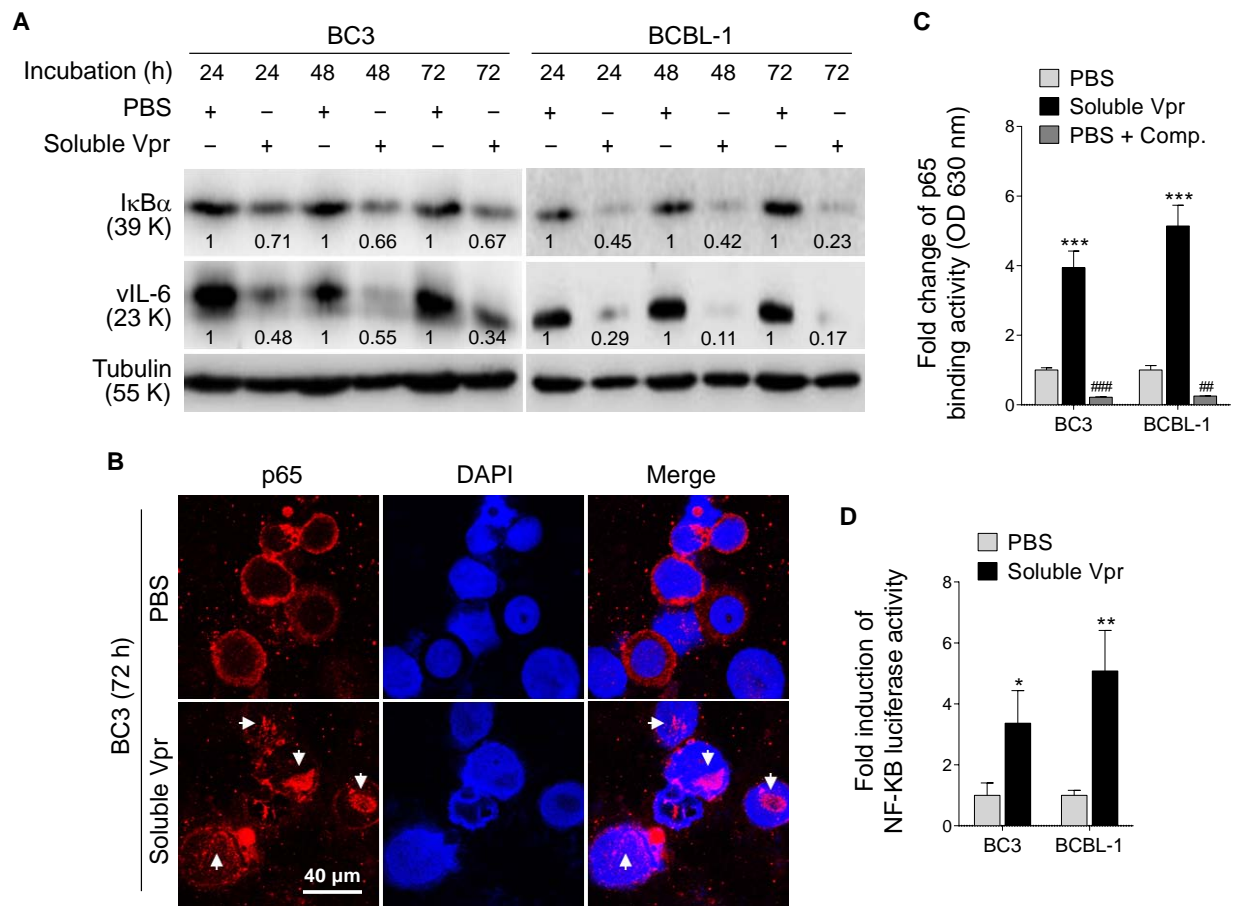


Figure 3

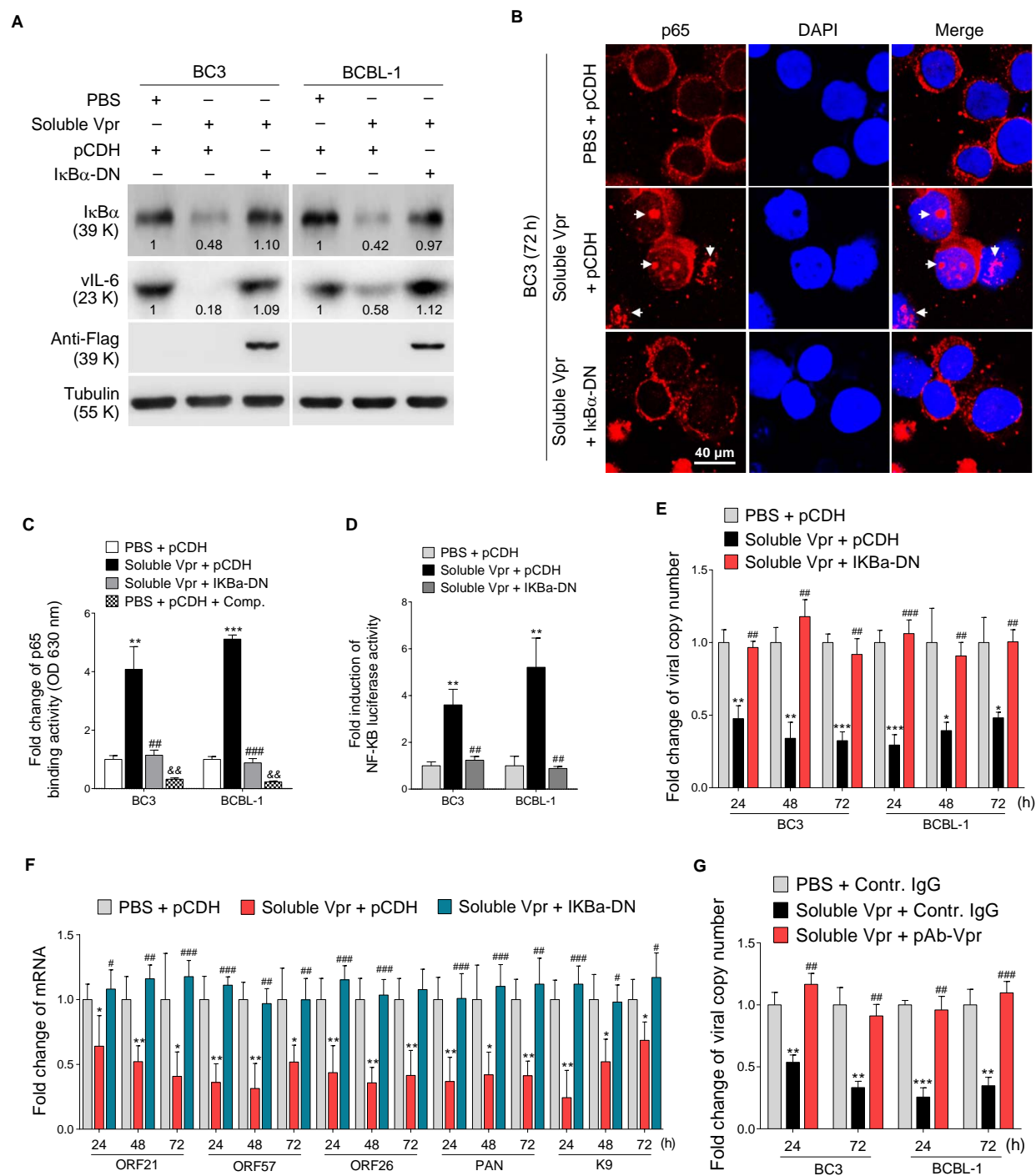


Figure 4

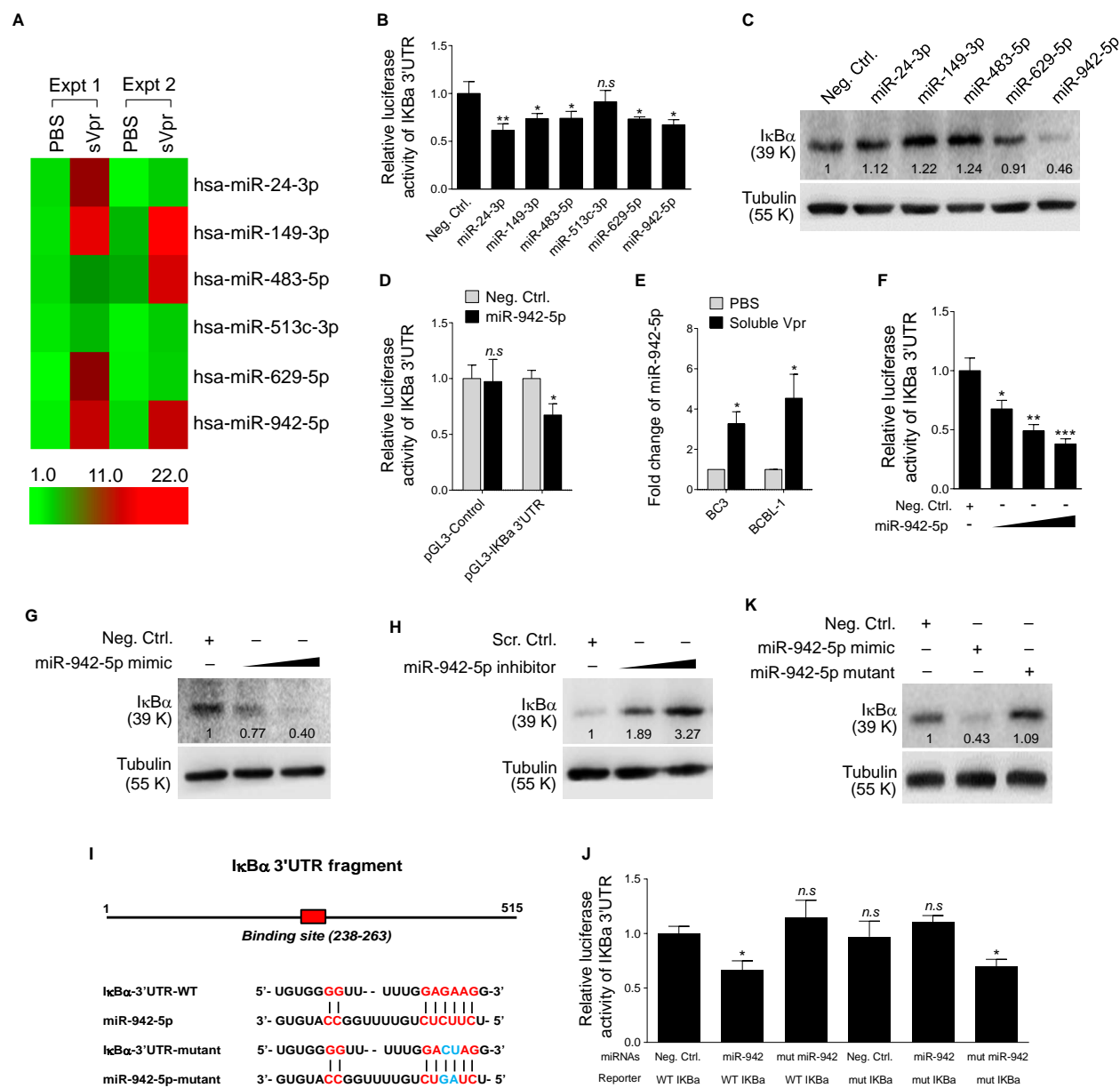


Figure 5

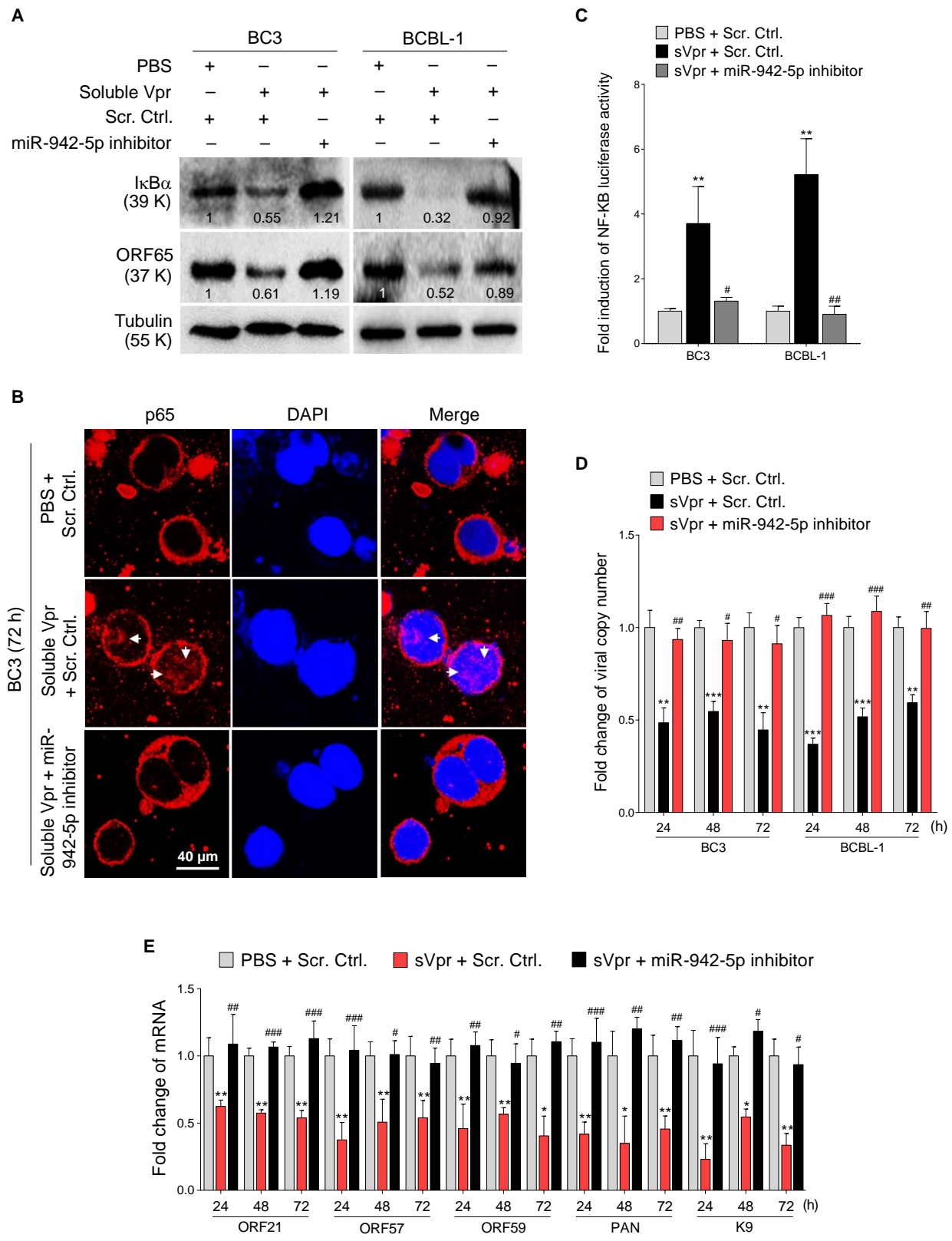


Figure 6

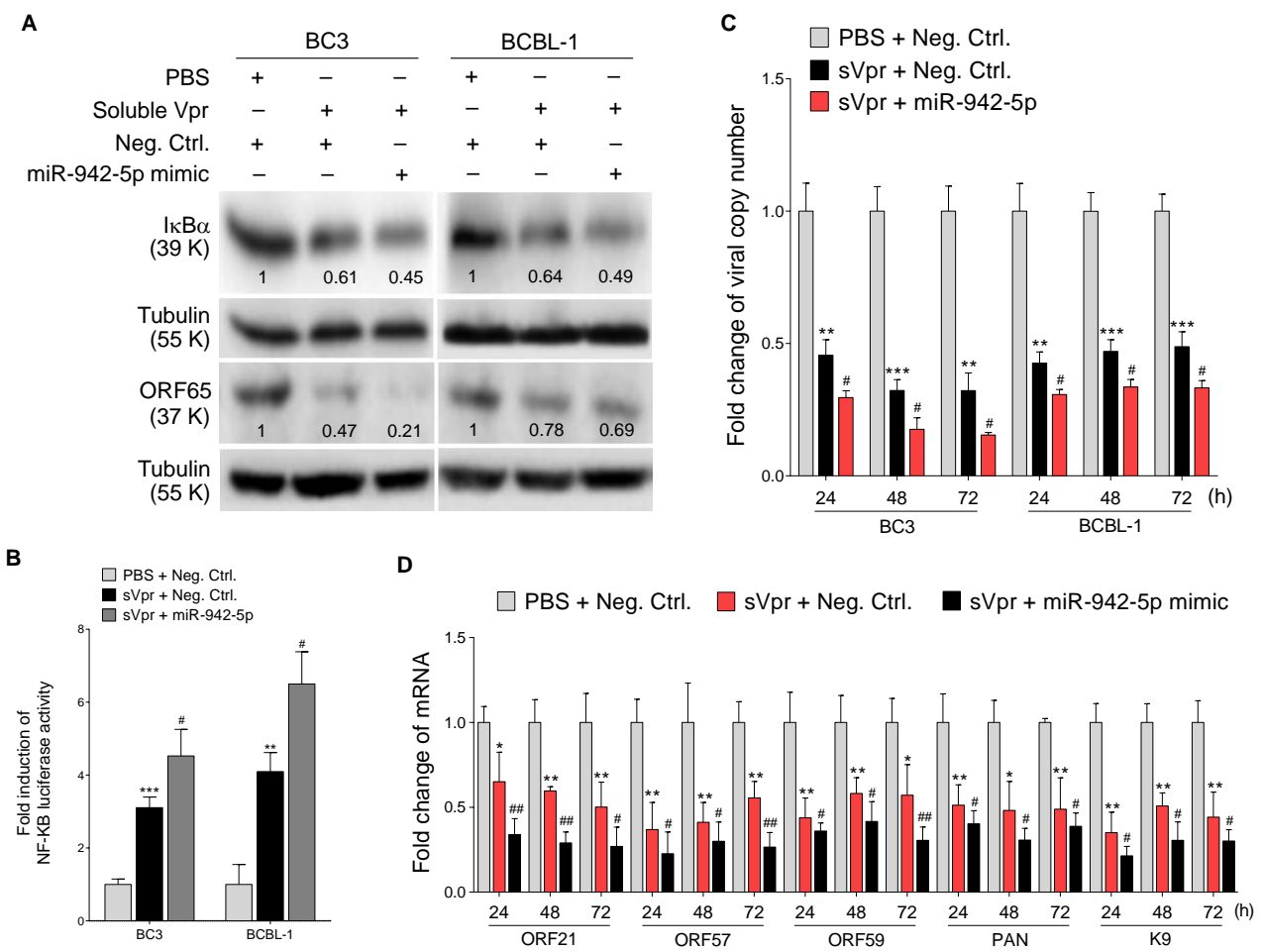


Figure 7

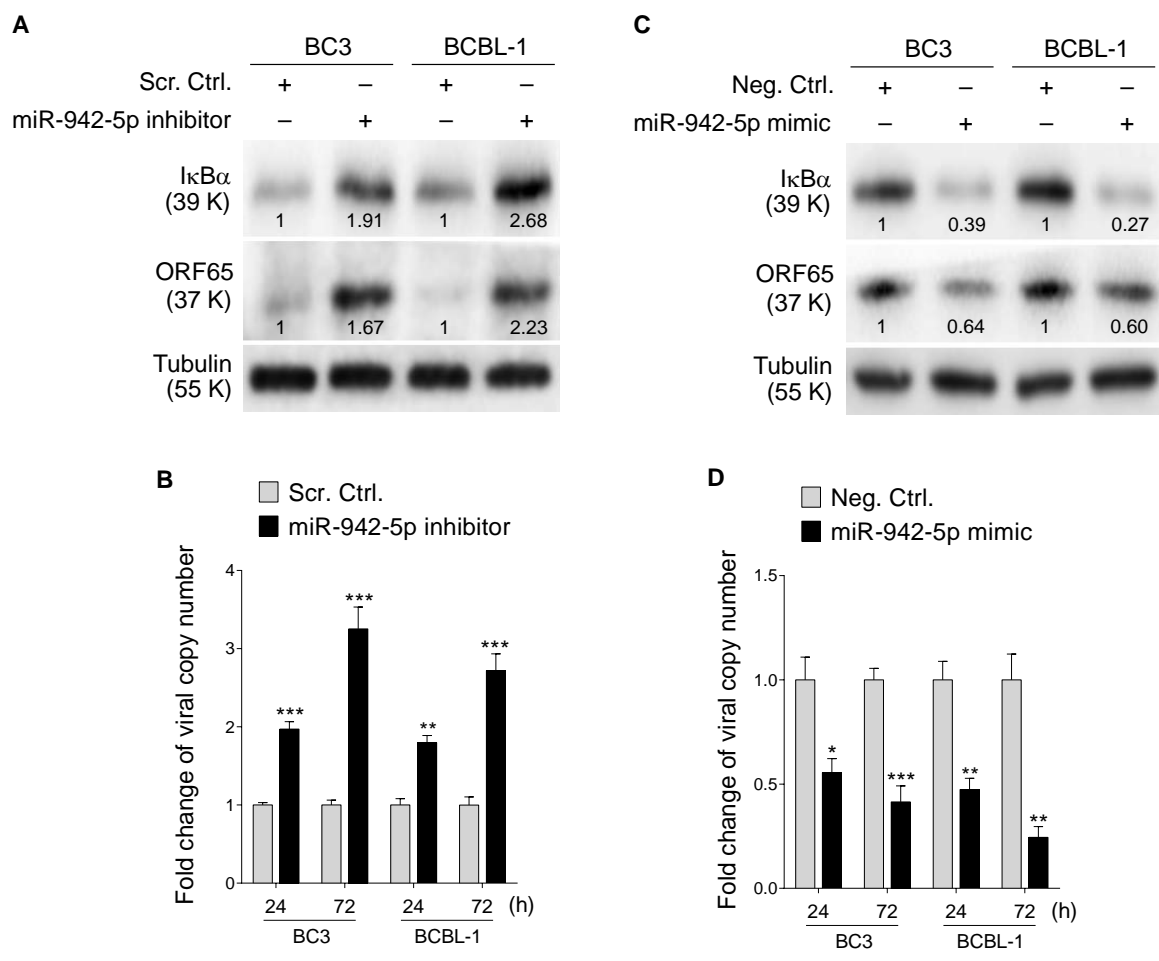


Figure 8